F. J. Leo

ANL-6705

ANL-6705

0456

Argonne National Laboratory

REACTOR DEVELOPMENT PROGRAM

PROGRESS REPORT

March 1963

LEGAL NOTICE

This report was prepared as an account of Government sponsored work. Neither the United States, nor the Commission, nor any person acting on behalf of the Commission:

A. Makes any warranty or representation, expressed or implied, with respect to the accuracy, completeness, or usefulness of the information contained in this report, or that the use of any information, apparatus, method, or process disclosed in this report may not infringe privately owned rights; or

B. Assumes any liabilities with respect to the use of, or for damages resulting from the use of any information, apparatus, method, or process disclosed in this report.

As used in the above, "person acting on behalf of the Commission" includes any employee or contractor of the Commission, or employee of such contractor, to the extent that such employee or contractor of the Commission, or employee of such contractor prepares, disseminates, or provides access to, any information pursuant to his employment or contract with the Commission, or his employment with such contractor.

ANL-6705
Reactor Technology
(TID-4500, 19th Ed.)
AEC Research and
Development Report

0456

ARGONNE NATIONAL LABORATORY
9700 South Cass Avenue
Argonne, Illinois

REACTOR DEVELOPMENT PROGRAM PROGRESS REPORT

March 1963

Albert V. Crewe, Laboratory Director

Division	Director
Chemical Engineering	S. Lawroski
Idaho	M. Novick
Metallurgy	F. G. Foote
Reactor Engineering	B. I. Spinrad
Remote Control	R. C. Goertz

Report coordinated by
R. M. Adams and A. Glassner

Issued April 15, 1963

Operated by The University of Chicago
under
Contract W-31-109-eng-38
with the
U. S. Atomic Energy Commission

FOREWORD

The Reactor Development Program Progress Report, issued monthly, is intended to be a means of reporting those items of significant technical progress which have occurred in both the specific reactor projects and the general engineering research and development programs. The report is organized in a way which, it is hoped, gives the clearest, most logical over-all view of progress. The budget classification is followed only in broad outline, and no attempt is made to report separately on each sub-activity number. Further, since the intent is to report only items of significant progress, not all activities are reported each month. In order to issue this report as soon as possible after the end of the month editorial work must necessarily be limited. Also, since this is an informal progress report, the results and data presented should be understood to be preliminary and subject to change unless otherwise stated.

The issuance of these reports is not intended to constitute publication in any sense of the word. Final results either will be submitted for publication in regular professional journals or will be published in the form of ANL topical reports.

The last six reports issued
in this series are:

September 1962	ANL-6619
October 1962	ANL-6635
November 1962	ANL-6658
December 1962	ANL-6672
January 1963	ANL-6683
February 1963	ANL-6698

TABLE OF CONTENTS

		Page
I.	Boiling Water Reactors	1
	A. BORAX-V	1
	1. Operations and Experiments	1
	2. Design, Fabrication, and Procurement	10
	3. Operator Training	11
II.	Liquid-metal-cooled Reactors	12
	A. General Research and Development	12
	1. Physics	12
	2. ZPR-VI Operation	14
	3. Preparations for ZPR-IX Operation	14
	4. Fast Reactor Fuels	15
	B. EBR-I, Mark IV	17
	C. EBR-II	17
	1. Reactor Plant	17
	2. Sodium Boiler Plant	20
	3. Power Plant	20
	4. Fuel Cycle Facility	21
	5. Fuel Development	23
	6. Process Development	26
	D. FARET	29
	1. Model Fuel Element (Zoned-core Test Zone) for Out-of-pile Tests	29
	2. Sodium Removal	29
	3. Physics	30
	4. Development of Ceramic Fuels	31
III.	General Reactor Technology	32
	A. Applied Nuclear Physics	32
	1. Recoil Counter for Fast-neutron Spectroscopy	32
	2. High-conversion Critical Experiment (ZPR-VII)	33
	3. Measurements of Flux Perturbation	34
	4. Sodium Absorption as a Spectral Index	35
	5. Theoretical Physics	37

TABLE OF CONTENTS

		Page
B.	Reactor Fuels and Materials Development	38
1.	Ceramic Fuels	38
2.	Corrosion Studies	43
3.	Nondestructive Testing	
4.	Development of Extrusion Techniques	46
C.	Chemical Separations	47
1.	Chemical-Metallurgical Process Studies	47
2.	Fluidization and Volatility Separations Processes	50
3.	Calorimetry	53
IV.	Plutonium Recycle Program	54
A.	Core Design	54
V.	Advanced Systems Research and Development	55
A.	Direct Conversion Studies	55
1.	Direct Conversion by Thermionic Emission with a Cesium Cell	55
2.	Thermionic Energy-conversion Diode with a Film-boiling Liquid Metal	56
3.	Nuclear Thermionic Power Systems	57
B.	Rocket Fuel Test Reactor (RFTR)	58
VI.	Nuclear Safety	63
A.	Thermal Reactor Safety Studies	63
1.	Metal Oxidation and Ignition Studies	63
2.	Metal-Water Studies	64
B.	Fast Reactor Safety Studies	64
1.	Meltdown Experiments with Ceramic Fuel	64
2.	In-pile Oxidation Studies	65
VII.	Publications	66

I. BOILING WATER REACTORS

A. BORAX-V

1. Operations and Experiments

a. Reactor Operations. In preparation for the core loading with central superheater, the nine control rods and the boiling core structure were transferred from the reactor vessel to underwater storage.

The third routine inspection of the control rods was completed after 65 Mwd of operation with the boiling cores. The rods were checked for thickness, angularity, straightness, and twist. All rods passed a 0.330-in. thickness gauge; all poison sections passed a 0.390-in. angularity gauge; and the followers passed a 0.438-in. angularity gauge. All rods were straight and had no twist greater than 0.025 in. All control rods passed the dimensional inspection and were within the design tolerances.

Control-rod drive seals and extension shafts were inspected and found to be in very good condition. Deposition of radioactive crud in the seal housing was negligible.

The original reactor vessel downcomer-flow and density-measuring probes were removed and replaced with larger probes. Modifications to external piping are being made to improve venting of this system.

The central superheater core structure was fitted with the flood-and-drain extension piping, perforated oscillator thimble, and samples to measure corrosion. The structure was installed in the vessel, and external superheat flood-and-drain piping was fitted and welded. Control rods and drives were reinstalled and checked out.

Loading of the boiling zone fuel for the core with central superheater was begun.

b. Transfer Function Analysis. Preliminary analysis of the transfer function measurements made with boiling core B-2, by means of the sine-cosine cross-correlation analog computer, has been carried out. The nomenclature used below corresponds to the following definition of the reactor transfer function:

$$G = \frac{\Delta n}{n_0 \Delta k} = \frac{G_0}{1 + G_0 H} ,$$

where G_0 is the zero-power transfer function, and H the feedback.

(i) Normalization of Power Transfer Functions. The differential worth of the rotating oscillator rod at power was determined indirectly by first measuring the flux amplitudes $\Delta n/n_0$ at the highest frequency (15 cps) studied, and then arbitrarily equating the gain of $G (= \Delta n/n_0 \Delta k)$ to the zero-power gain at this frequency. Thus, the deduced worth equals the observed amplitude divided by the gain of the zero-power transfer function at the normalizing frequency. The assumption of the presence of no feedback at 15 cps is certainly open to question in the case of BORAX-V. There is evidence that some feedback is still present at this frequency, particularly at the higher powers.

The gain of the observed transfer function G was determined simply by dividing the measured flux amplitude at each frequency by the reactivity amplitude as determined above. The phase of the observed transfer function, ϕ_G, was obtained by normalizing to the zero-power phase at the highest frequency studied. Thus, a phase-correction term was added at each frequency.

(ii) Reactor Transfer Function G. The gain and phase of G at various powers are shown in Figure 1. The curves are characteristic of boiling water reactors having long thermal time constants, except for the high-gain and high-phase lead below one cycle per second. Preliminary analyses show this effect can be due either to a very high gain in the void feedback loop or to very short thermal time constants (less than 0.1 sec). Since the latter case is not possible for BORAX-V with its low value of thermal conductivity for UO_2, a high void-reactivity coefficient is indicated.

The resonant frequency increases with power due to the increasing feedback gain. The resonance peak also increases with power as expected. It was found that the overall reactor response cannot be well approximated in the resonance region with a quadratic transfer function. Figure 1 shows that the resonance gain approaches 5 db at 16.5 Mwt.

(iii) Open-loop Transfer Function G_0H. The response of G_0H was calculated for the various power runs, and the results are shown in the Nyquist diagram of Figure 2. In this case, only the results for higher frequencies are shown. At lower frequencies, the curves continue into the fourth quadrant as expected. Some inconsistencies are indicated near the origin (at high frequencies) as to whether or not the reactor could go unstable at very high power. In Figure 2, lines have been drawn through the curves for five power runs, linking points with common frequencies in the range from 2.0 to 0.85 cps.

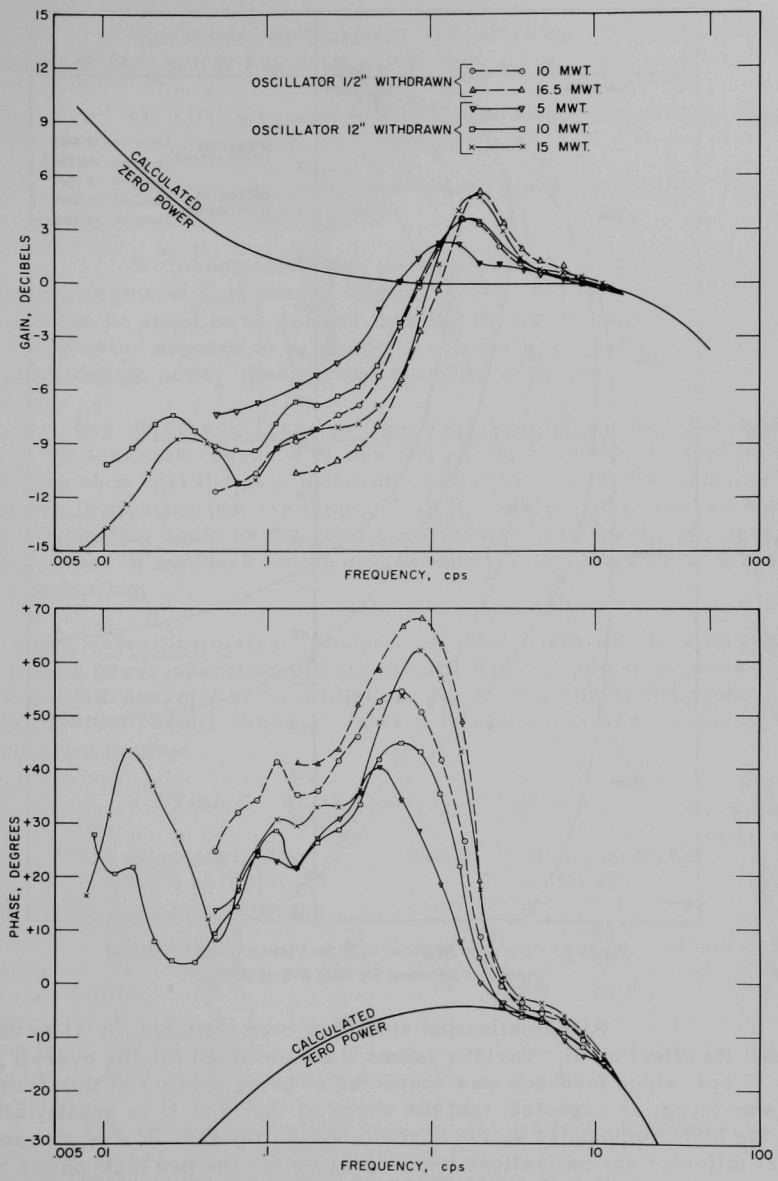

Figure 1. Gain and Phase vs. Frequency for Various Power Levels and Oscillator Insertions for Core B-2 of BORAX-V

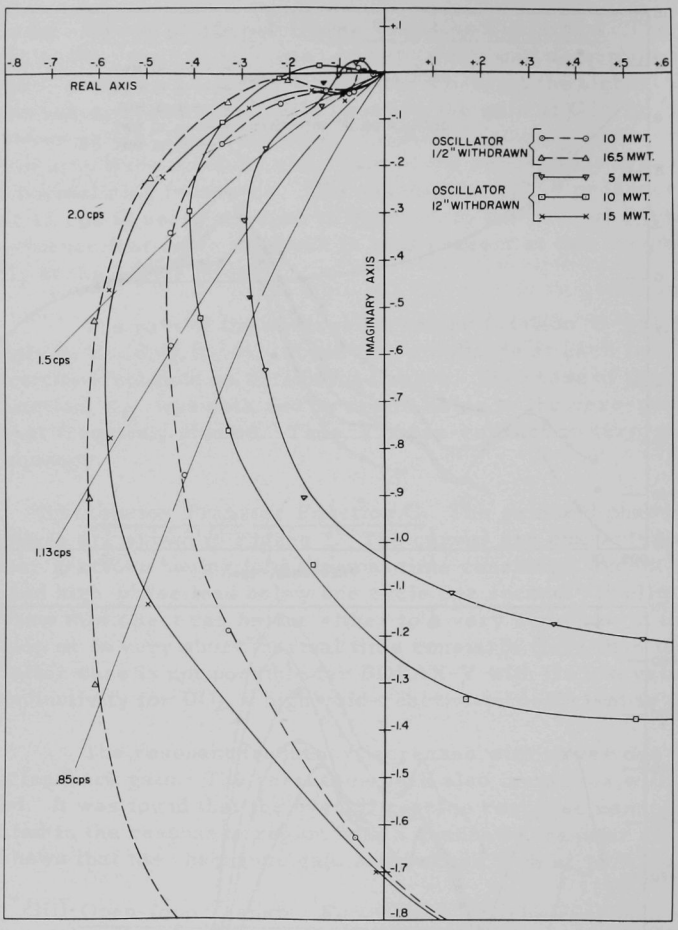

Figure 2. Open-loop Response G_0H for Various Power Levels and Oscillator Insertions for Core B-2 of BORAX-V

A normalization study has been initiated for G to determine its effect on H. Various values were assumed for the overall gain at 15 cps, since feedback was suspected of being present at this frequency. It was found, as expected, that the shape of G_0H and H is greatly affected at the high frequencies by the normalization imposed. It was also found that different normalizations were required for the two high-power runs to deduce comparable feedback functions for both. It is suspected that this effect was due to the large power oscillations induced during the 16.5-Mwt run.

The above study showed that, at 15 cps, the most reasonable G_0H and H transfer functions resulted if

(1) $|G|$ was assumed to be somewhat higher than $|G_0|$, but less than 10% higher, and

(2) ϕ_G was assumed to be somewhat lower than ϕ_{G_0}, but less than 6° lower.

With normalizations performed in the above range, gain and phase margins of G_0H for the highest power runs (16.5 and 15 Mwt) were found to be equal to or greater than 8.0 db and 50°, respectively. Thus, the reactor appears to be stable at powers in excess of the maximum plant-design power-dissipation capability of 40 Mwt.

(iv) Feedback Transfer Functions Results H. The gain and phase of the feedback response H are plotted vs. frequency in Figure 3. The curves show that the gain increases somewhat faster than linearly with power, indicating that the void-reactivity coefficient increases with power. Depending again on the normalization assumed for G, the results show the order of feedback function to be equal to or greater than a net second-order lag.

c. Water Chemistry. Analysis of water chemistry measurements made during power operation of boiling core B-2 continued. A mass-spectrographic analysis of the radiolytic gas from a condensed steam sample gave the results shown in Table I, in which they are compared with an absorption method.

Table I. Water Chemistry Analysis

Mass Spectrographic Analysis, % by Volume		Blacet-Leighton Analysis, % by Volume	
H_2	- 52.8	H_2	- 56.6
O_2	- 33.4	O_2	- 32.4
N_2	- 12.4	Inerts	- 11.0
A	- 0.27		
CO	- ~1.0		
CO_2	- 0.2		

The absorption method used did not distinguish between CO, CO_2, and O_2, or CO, CO_2, and H_2. Reasons for the difference in results between analyses is the inherent ± 2% error of the Blacet-Leighton method and the fact that these analyses were made on different samples. All things considered, the results are in fair agreement.

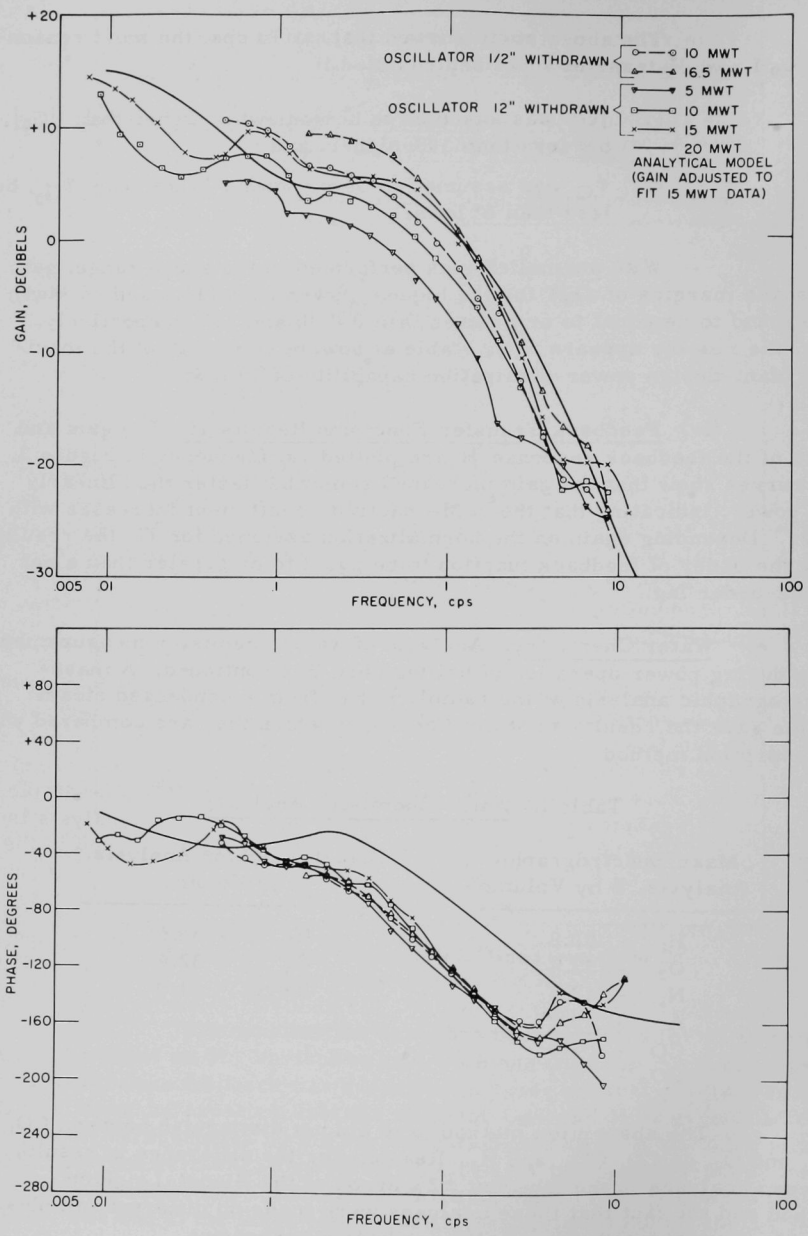

Figure 3. Gain and Phase of Feedback H for Various Power Levels and Oscillator Insertions for Core B-2 of BORAX-V

Emission-spectrographic analyses of suspended solids from the reactor water are shown in Table II.

Table II. Emission-spectrographic Analysis of Suspended Solids for Sample Period 1/16/63 - 1/18/63

Element	Concentration, %	Element	Concentration, %
Al	>5.0	Co	<0.1
Fe	>5.0	Mg	<0.1
Cr	~1.0	Mo	<0.1
Ni	~1.0	Si	<0.1
Cu	~0.1	Sn	<0.1
Mn	~0.1	Ti	<0.1
Pb	~0.1	Zn	<0.1

An X-ray-spectrographic analysis was also made but was not successful in identifying all the components of the suspended solids. An "as-filtered" sample was examined, but, due to the amorphous character of the material, only α-Fe_2O_3 and Fe_3O_4 could be found. Although FeC was identified, its X-ray spectrum is similar to that of mica. Since mica is very likely present from broken sight-glass incidents, the identification of FeC is questionable.

During the operation of the boiling cores, sample streams were passed through resin columns for various purposes. The exhausted resins were saved and later eluted to get an idea of the various elements found in solution. The resulting eluent was quite concentrated; consequently, several elements were easily found which had not been detected in a sample of unconcentrated reactor water. The emission-spectrographic analysis is given in Table III, along with the approximate concentrations found in the eluent.

Table III. Emission-spectrographic Analysis of Eluent from Resin Column

Element	Concentration	Element	Concentration
B	>1.0 mg/ml	Ni	0.2 mg/ml
Al	0.2 mg/ml	Si	0.08 mg/ml
Ca	4.5 mg/ml	Cu	Trace
Cd	0.1 mg/ml	Ga	Trace
Cr	0.1 mg/ml	Pb	Trace
Fe	0.2 mg/ml	Na	Trace
Mg	0.3 mg/ml	Sr	Trace
Mn	0.5 mg/ml	Ba	Trace

Work on the BORAX-V radiolytic gas recombiner has resumed. A new Knallgas generator design has been approved and is presently being constructed. All safety equipment for the recombiner is on hand and has been partly installed.

d. In-vessel Instrumentation

(i) Fuel Temperatures. In addition to the fuel-temperature data tabulated in Progress Report for February 1963, ANL-6698, p. 7, selected fuel temperatures, as a function of integrated power, are illustrated in Figure 4.[1] The rising temperatures appear to be an indication of an effect of small amounts of fuel irradiation.

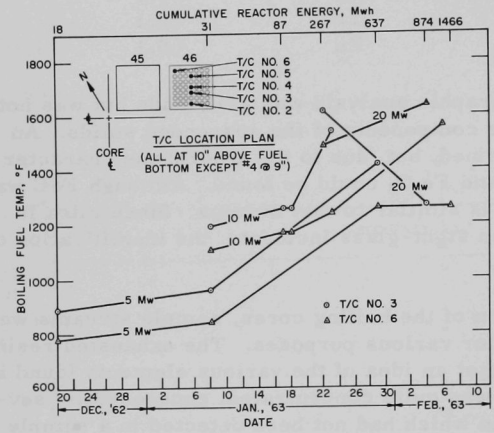

Figure 4

Boiling Fuel Temperature vs. Operating Date at Fixed Reactor Power Levels for Core B-2 of BORAX-V

To help separate the effect of possible irradiation damage to the W-W/26% Re thermocouples from the effect of an apparent decrease in the thermal conductivity of the UO_2 fuel, three different reactor scram tests were performed in which all fuel thermocouple outputs were recorded. Figures 5 and 6 show the results for two representative thermocouples, and the 63.2% time constants obtained from same are tabulated in Table IV. All time constants are based on the fuel temperature reaching the reactor water temperature of 489°F in due time.

---

[1] The correct orientation of the instrumented fuel assembly is shown in Figure 4. Figure 2, page 8 of ANL-6698 incorrectly shows the orientation which truly has fuel rods No. 1 and 49 along a north bearing.

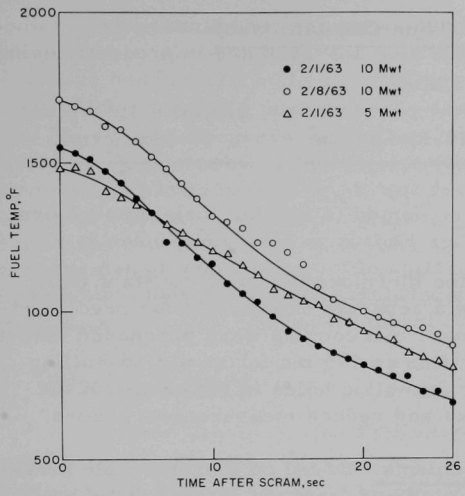

Figure 5

Scram Tests T/C No. 3 - Boiling Fuel Temperature vs. Time after Scram - BORAX-V

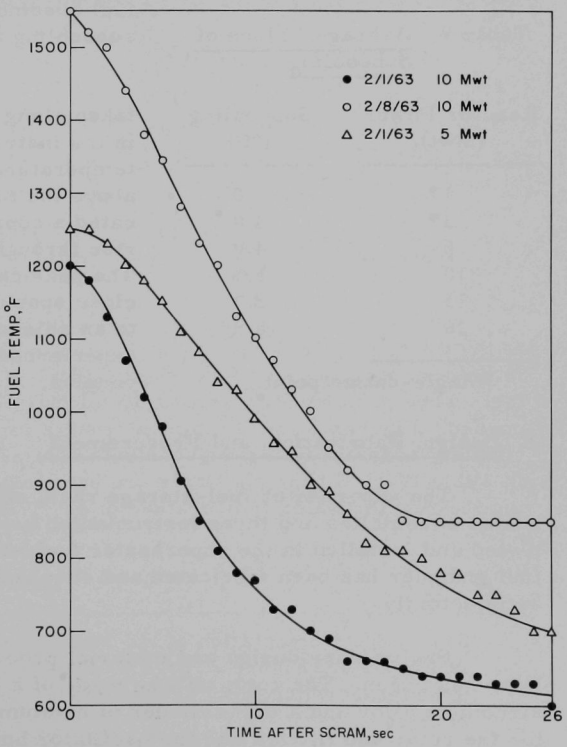

Figure 6

Scram Tests T/C No. 6 - Boiling Fuel Temperature vs. Time after Scram - BORAX-V

Table IV. 63.2% Time Constant (sec)

	2/1/63 - 763 Mwht		2/8/63 - 1503 Mwht
	5-Mw Scram	10-Mw Scram	10-Mw Scram
T/C No. 3	24	15	23
T/C No. 6	21	10.5	17

The separation of the thermocouple time constant from the fuel time constant would involve a separate experiment for precise information and has not been performed. All couples were purchased with a maximum 63.2% time constant specified as 175 ms for an air-to-boiling water test. They are spring loaded into blind holes in the center of the fuel pellets to further assure contact and reduce measurement errors.

(ii) Subcooling Measurements. Based on thermocouple measurements of the water temperature obtained from the instrumented boiling fuel assembly, the averaged values of subcooling are indicated in Table V.

Table V. Average Values of Subcooling

Reactor Power (Mwt)	Subcooling (°F)
1*	3.0
3*	4.0
5	4.0
10	5.9
15	6.0
20	8.0

*Single-datum point.

Other water temperatures taken along the axis of a coolant channel in the instrumented assembly showed a temperature peak at a distance of 6 in. above the fuel base, but otherwise indicated a constant rate of temperature rise throughout the length of the fuel. The peak can be attributed to the too-close spacing of that thermocouple to an adjacent fuel rod. Difficulty was experienced in the alignment of these couples.

2. Design, Fabrication, and Procurement

The superheater fuel-storage rack, capable of storing 23 superheater assemblies and three instrumented boiling assemblies, was completed and installed in the superheater fuel-storage tank. The superheat fuel grappler has been fabricated and checked out, and is operating satisfactorily.

Preliminary design and material procurement for a fueled oscillator has begun. The rotor will be made of a half cylinder of uranium-zirconium alloy and a half cylinder of hafnium. Zircaloy-2 will be used for the rotor end fittings and the oscillator housing.

The acoustic reactor water-level-measuring device designed and fabricated by Aeroprojects, Inc. has been delivered.

Pieces from a portion of the depleted Type 406 stainless steel-clad fuel plates (see Progress Report for January 1963, ANL-6683, p. 5) were received from Atomic International for evaluation. The clad-to-clad bond, achieved by electropolishing picture frames and cover plates, and hot evacuation of the rolling compact, is greatly improved over the bond achieved during the initial fabrication development done by AI on depleted Type 406 stainless steel-clad plates. Although grain growth had taken place across interfaces, vestiges of mating lines remained in the form of discontinuous inclusions.

3. Operator Training

Another session of the BORAX-V systems training course was begun for technicians who have not previously taken this course. Two of the classes have been attended by all operating personnel for retraining on health physics procedures and on details of the control console, recorder panel, and electrical controls.

II. LIQUID-METAL-COOLED REACTORS

A. General Research and Development

1. Physics

a. ZPR-III

(i) Theoretical Analysis. There is a very large incentive to learn how to study as many of the properties as possible of very large fast power-breeder reactors by setting up a relatively small fraction of the large reactor as the central zone of a multiple-zoned reactor. The system will consist of a small fraction of the large reactor core as the central zone which is surrounded by a more reactive driver zone. There may also be a buffer or filter zone installed between the two principal regions.

As a first step in studying this concept, an essentially "known" system was proposed for experiment. The composition of ZPR-III Assembly 42 (see Progress Report for January 1963, ANL-6683, p. 7) was selected for the central zone which had been previously studied and is somewhat representative of a 500-liter uranium monocarbide reactor. The proposed driver partially resembled ZPR-III Assemblies 12, 14, and 17. The primary objective in selection of the driver and filter composition is to achieve the best possible spectral matching of the real and adjoint fluxes at the center of the multiple-zoned core to that of the single-zone core, so that central spectra could be determined and central reactivity coefficients for the central core might be measured. A second objective was to achieve this spectral matching over as much of the central zone as possible. This would be important for Doppler effect and sodium void coefficient studies.

Table VI gives the normalized real and adjoint spectra of the single-zone Assembly 34[2] and of the two-zone system with the Assembly 34 material as its central zone material. It can be seen that even as far out as 17.6 cm of the 23.5-cm central zone a rather satisfactory match has been achieved.

The next step in the analysis will be to try to extend this technique to a central zone representative of a large power-breeder system.

(ii) Reactivity Worths of Axial Columns of Reactor Material at Various Radii. In order to allow for accurate calculation of the reactivity effects of reactor material as a function of radius, various materials of interest were measured in Assembly 42 at specific radii, distributed over the full axial length of the core and driver. Measurements were made at three different radii in the core and one in the driver.

---

[2] R. J. Huber *et al.*, ANL-6401

Table VI. Comparison of Real and Adjoint Fluxes for Two-zone Mockup of Assembly 34

Group	E_L, Mev	Assembly 34 as One-zone Real Flux		Assembly 34 as Two-zone Real Flux		Assembly 34 as One-zone Adjoint Flux		Assembly 34 as Two-zone Adjoint Flux	
		r = 0	r = 17.6 cm	r = 0	r = 17.6 cm	r = 0	r = 17.6 cm	r = 0	r = 17.6 cm
1	3.67	0.0186	0.0186	0.0187	0.0192	0.0616	0.0620	0.0629	0.0659
2	2.23	0.0371	0.0370	0.0370	0.0372	0.0610	0.0613	0.0620	0.0647
3	1.35	0.0676	0.0674	0.0671	0.0662	0.0581	0.0583	0.0588	0.0607
4	0.825	0.1041	0.1036	0.1035	0.1029	0.0539	0.0539	0.0542	0.0546
5	0.5	0.1421	0.1416	0.1424	0.1432	0.0549	0.0548	0.0550	0.0552
6	0.3	0.1513	0.1511	0.1521	0.1526	0.0579	0.0577	0.0579	0.0581
7	0.18	0.1297	0.1298	0.1303	0.1305	0.0601	0.0599	0.0601	0.0601
8	0.11	0.0970	0.0972	0.0977	0.0989	0.0622	0.0619	0.0620	0.0617
9	0.067	0.0793	0.0795	0.0796	0.0792	0.0632	0.0630	0.0630	0.0627
10	0.041	0.0685	0.0689	0.0685	0.0681	0.0641	0.0639	0.0638	0.0636
11	0.025	0.0336	0.0338	0.0336	0.0341	0.0656	0.0654	0.0652	0.0648
12	0.015	0.0364	0.0367	0.0359	0.0349	0.0662	0.0660	0.0658	0.0656
13	0.0091	0.0181	0.0183	0.0177	0.0174	0.0682	0.0682	0.0677	0.0668
14	0.0055	0.00718	0.00724	0.00698	0.00699	0.0684	0.0685	0.0679	0.0665
15	0.0021	0.00776	0.00782	0.00748	0.00731	0.0683	0.0684	0.0678	0.0658
16	0.0005	0.00149	0.00149	0.00142	0.00137	0.0664	0.0666	0.0660	0.0632

The reactivity measurements were performed by comparing the critical rod positions with full-density aluminum, and then with 45% aluminum in the sample columns. The aluminum worth was determined from the difference in critical rod positions and the aluminum mass change between the two runs. A reference core having these sample columns voided was then calculated from the aluminum worth. This reference core was used as a basis for determining the reactivity effects of columns of graphite, stainless steel, and depleted uranium.

The reactivity effect of a column of enriched uranium was determined by replacing a $\frac{1}{8}$-in.-thick column of diluent with a $\frac{1}{16}$-in. column of enriched uranium and a $\frac{1}{16}$-in. column of 100% aluminum. The previously determined worth of aluminum and diluent were used in association with the change in critical rod position to determine the worth of the added enriched uranium. The reactivity worths of these materials are given in Table VII. For U^{235} and U^{238}, the values have been calculated from the enriched and depleted worths.

Table VII. Radial Distribution of Worth of Axial Columns of Reactor Materials

Material		Radius (in.) R = 0	R = 4.875	R = 6.89	R = 11.75
Aluminum	Ih/kg	3.5	3.7	3.7	6.7
	Ih/column (100%)	0.63	0.67	0.67	1.2
Stainless Steel	Ih/kg	0.12	0.45	0.43	2.6
	Ih/column	0.06	0.22	0.21	1.3
Graphite	Ih/kg	29.4	27.4	23.8	23.0
	Ih/column	3.2	3.0	2.6	2.5
U^{238}	Ih/kg	-2.7	-2.5	-2.2	-0.42
	Ih/column (depleted)	-3.2	-3.0	-2.6	-0.49
U^{235}	Ih/kg	79.0	78.0	72.0	39.7
	Ih/column (enriched)	45.0	45.0	41.0	23.0

(iii) Nuclear Track Emulsion Exposures. Several irradiation runs were made in which 400-μ-thick Ilford E-1, 100-μ-thick Ilford L-4, and 100-μ-thick Gevaert 307 emulsions were exposed to total integrated fluxes ranging from 1×10^8 to 10^9 nvt. Twenty-one emulsion packets, representing seven of each type, were sent to Northwestern University for analysis. Nine minature Ilford L-4 cadmium-covered emulsion packets were sent to Centre d'Etudes de l'Energie Nucleaire, Mol-Donk, Belgium.

(iv) Sodium, Enriched Uranium, and Natural Uranium Irradiations. Capsules, containing sodium and natural and enriched uranium foils, were irradiated at points along the axial and radial reactor midlines. All of the foils were irradiated during a single 50-watt-hour run. Analyses are now being performed.

(v) Assembly 43. The latter part of the month was devoted to maintenance and preparation of the facility for Assembly 43. The control rods were repositioned in a radial direction, and amphenol disconnect fittings were installed in the power cables of the five control rods in Half No. 2 to provide for easy removal of the drive mechanisms.

Additional monitoring and control equipment was added to the control circuit to prevent movement of the carriage in a wrong direction ("in" instead of "out") due to single phasing of the three-phase motor or phase reversal. A phase-reversal monitor was installed for the three-phase power circuits of the carriage and rod drive motors, and wiring was completed for a loss-of-phase monitor. The drive clutch and main thrust bearing were disassembled, inspected, and reassembled and adjusted.

Preliminary calibrations of a 4π absolute beta counter and scintillation well counter have been established with a sodium sample irradiated in CP-5. Loading of inert materials for this assembly was completed by the end of the month.

2. ZPR-VI Operation

The non-nuclear testing of the ZPR-VI facility has been completed. Approval for operation has not yet been received from the AEC, although the Reactor Safety Analysis Report was submitted in August, 1962.

3. Preparations for ZPR-IX Operation

The ZPR-IX facility is now scheduled to be used for a series of critical experiments in connection with the nuclear rocket reactor program. Listed below are some of the items which are being done to prepare the facility for operation.

Welding difficulties were experienced in assembling the aluminum matrix tubes into 5 by 5 arrays. By the elimination of tack welding and the use of spot welding only, the amount of distortion caused by the welding heat can be reduced. The lateral pressure applied by the holding knees should correct the distortion in this direction. The weight of the loading should flatten the bundles in the vertical direction.

Preparations are underway to test the matrix tubes with a hydraulic press. These tests will be similar to some conducted previously, but will be extended in three ways. First, measurements will be made, not only of the total deflection in the press, but in the top and bottom of the tube, which could cause control rod binding. Second, tests will be made with the sides of the tube free and also with the sides constrained from bulging outward, as they would tend to do in the actual matrix assembly. Finally, each matrix tube will be loaded to an assumed maximum (equivalent to more than an 8-ft-high column of solid uranium) and then unloaded to measure yield before being reloaded to destruction.

A shipment of aluminum drawers which are to be loaded with fuel prior to inserting in the matrix tubes has been received from the vendor and is being inspected. Two drawers will be filled with a typical loading composition and spacer springs to determine the effect of spring pressure on the drawer ends.

The control console and instrumentation tests have been completed, and a test report summarizing the results has been issued.

The remaining dual-purpose safety and control rod drives required for the ZPR-IX facility are now being assembled. Individual testing of the drives will begin next month.

4. Fast Reactor Fuels

a. Corrosion of Fuel-cladding Materials for Sodium-cooled Reactors. Three vanadium-base alloys which were tested in flowing sodium (~2 fps) at 650°C and identical untested samples have been analyzed for oxygen. Microhardness measurements (see Progress Report for February 1963, ANL-6698, p. 13) of the tested specimens had shown the edge hardness to be much greater than the center hardness, whereas the as-received samples showed no such variation. The test samples of all three alloys showed a characteristic surface layer which differed from their matrix material. The results of the oxygen analysis are given in Table VIII.

An electron diffraction study was unsuccessful in determining the structure and identity of the surface layer. X-ray powder patterns have been taken on the V-5 Ti-20 Nb test sample. These show two sets of diffraction lines. One set has been identified as the base material (V-5 Ti-20 Nb); the other set has not been identified. The lines do not correspond to any of the simple oxides of the constituents present and therefore it is suggested that it is a complex mixed oxide.

Table VIII. Oxygen Pickup by Vanadium Alloys Exposed to Sodium

Sample Composition (w/o)	Oxygen Content, ppm			
	As-received		Tested	
	(1)	(2)	(1)	(2)
V-10 Ti-3 Nb	640	690	1300	1500
V-10 Ti-3 Ta	590	550	1800	1800
V-5 Ti-20 Nb	590	510	1200	1200

(b) Nondestructive Tests on Stainless Steel-Vapor-deposited Tungsten Tubing. This tubing is standard Type 304 stainless steel tubing of EBR-II Core I jacket size in which an approximately 0.00075-in.-thick layer of tungsten is deposited on the inner surface. The tubing is being used in experimental fast reactor development studies. It was tested by pulsed electromagnetic test equipment which indicated that a considerable number of defects existed in most of the tubes. Metallographic sections at some of these locations showed that the tungsten layer appeared somewhat previous, with at least some narrow crack-like passages completely through it. At other spots the tungsten appeared to be separated from the stainless steel by variable amounts. This probably accounts for the bulk of the defect signals.

(c) Penetration of Stainless Steel by Molten Uranium and U-5 w/o Fs. Penetration rate studies of molten uranium and U-5 w/o Fs through Type 304 stainless steel are being performed in the TREAT reactor as an extension of some furnace experiments to more closely duplicate actual reactor conditions.

Six experiments, one with molten uranium and the others with the molten alloy, have been completed in the temperature range from 1100 to 1300°C. Each consisted of one sodium-bonded fuel rod and one unbonded rod. The unbonded rods gave erratic results making it difficult to determine penetration times. For the less severe transients of the sodium-bonded rods, penetration times for 9-mil clad were found to be about 2.0 sec, whereas times for the more severe transients were about 1.1 sec. The intermediate transients produced times of about 0.7 sec. The most severe transients caused failure almost instantly, but previous calculations indicated that this could be caused by bursting of the clad owing to internal pressure buildup. The results of these TREAT tests are in good agreement with the earlier furnace experiments covering the same temperature range.

B. EBR-I, Mark IV

Traverse activation of metallic foils of depleted uranium in the outer blanket for the purpose of breeding gain measurements was completed. It is suspected that the inability to resolve a pure Np^{239} component from the depleted uranium monitor foils irradiated in a thermalized graphite position, reported in Progress Report for February 1963, ANL-6698, p. 16, may be due to an impurity in the foils with a high thermal cross section.

To establish the patterns of Pu^{239} production, monitor foils were irradiated at the outer edge of the inner blanket. No difficulty was encountered with separation of a pure Np^{239} component in the depleted uranium foils located in the reactor core or blanket positions. The irradiations for breeding gain measurements were completed by irradiating foils of U^{235}, U^{238}, and Pu^{239} at the reactor center for radiochemical analysis.

The reactor was reloaded for power operation, and the oscillator rod was installed. With period measurements over a complete revolution, the oscillator rod was found to be worth 17 inhours. With additional fuel added for high-temperature operation, the reactor is now critical at room temperature with the lead cup blanket at 2.5 in. Low-power operation of the reactor with oscillator has begun.

C. EBR-II

1. Reactor Plant

The amounts of deflection and of rotation of the primary tank cover with variations in the temperature in the primary tank are important to the operation of (1) the fuel-handling mechanisms; and (2) the integrity of the seal (trough) of the large rotating plug.

As stated in previous reports (see, for example, Progress Report for April 1962, ANL-6565, p. 20), a temperature differential will exist across the primary tank cover structure when the temperature of the primary tank is elevated. A downward bow in the cover will result from the temperature differential which, in turn, tends to tilt the cover nozzles which project into the tank. Thus, the lower ends of the nozzles and the mechanisms located therein tend to move slightly both outward and radially. Measurements were made of the cover movements prior to filling with sodium at a tank temperature of about 325°F. These measurements indicated radial rotations, or tilt, of the hangers and various nozzles to be generally less than predicted for the measured temperature differentials.

Recent measurements made with the primary tank filled with sodium also indicate that the actual cover rotations and deflections are less than the calculated values. These measurements were made at several temperature levels of the tank up to 650°F. Included in these data are measurements of the radial (outward) displacement of the cover at the six hangers,

rotation (or tilt) of the cover at the six hangers, and the vertical displacement of the cover at six locations near the center ring (including three locations in the large rotating plug seal trough).

Of the two types of measurements made, namely, rotation and deflection, the former are more reliable simply because they give the actual angle of rotation directly, whereas the deflection readings must be corrected for temperature variations at different locations in the cover. In the case of the vertical displacement of the large rotating seal trough, however, simple direct measurements are made of the movements, and hence these readings accurately define the position of the seal trough at all temperature levels.

In general, the rotation measurements indicate that the actual angles of rotation are 25% less than the calculated values for a given measured temperature differential across the cover, whereas the observed vertical displacements (deflections) are about 35% less than the calculated values.

In addition, it was determined from the present readings as well as from previous tests that the radial (outward) thermal growth of the cover occurs in a uniform fashion about the vertical centerline of the tank. Therefore, it is concluded that the method of supporting the primary tank (from six hangers, spaced at 60° intervals around the periphery of the cover, bearing on high-strength steel rollers) does, in fact fulfill the design objectives, namely, to support the tank in such a fashion as to minimize or eliminate expansion stresses, and to maintain the concentricity of the primary tank vertical centerline and the large rotating plug centerline at all times.

Heating of the primary tank sodium above the 275°F filling temperature was initiated. By the end of the month, the temperature had been raised in 50°F steps to 650°F. The temporary cold trap for the primary system had been maintained in continuous operation during the heat-up.

When the heat-up started, the shield-cooling system was placed in operation, and exhaust flow increased as the bulk sodium temperature was increased. Adjustments were made to provide proper flow and air distribution as required to meet the changing conditions due to temperature changes of the bulk sodium. Currently, the 40-ton shield-cooling refrigeration unit is also in operation at reduced load. The thimble-cooling system has been in continuous operation throughout the month. Adjustments to the flow distribution were made as necessary to provide sufficient cooling to all instrument thimbles.

Before raising the temperature of the bulk sodium, the permanent argon system was connected to the primary tank and the silicone system, which cools the argon, was also put into operation.

From the time the temporary sodium-purification system was put into operation, troubles were experienced with the plugging indicator and the sodium-sampling valve. Two sodium samples were taken: one at a bulk temperature of 400°F, and one at 450°F. These showed an expected rise in concentrations of iron, chromium, nickel, and molybdenum. Because of ambiguous plugging-indicator data, in contrast with the excellent results obtained with the secondary system, it was decided to move the secondary system distillation apparatus to the temporary system to get additional samples. Earlier problems with the sampling valve reoccurred, and the sampling valve plugged tightly, precluding the use of the distillation apparatus or the taking of samples from the primary system.

Present efforts are directed toward remodeling the surge tank on the permanent purification system so that this system can be filled and its plugging indicator and sample facilities used.

The temporary cold trap has been run so that the outlet of the crystallizer tank has been maintained at 325°F while the coldest spot in the crystallizer tank has been 270°F. Thus, cold trapping has been taking place, and it is believed that the plugging temperature is below 400°F (approximately 30 ppm sodium oxide).

At 650°F, the reactor vessel cover was raised and the primary auxiliary electromagnetic pump was tested for 24 hr with the use of rectifier power. The cover was lowered after this test was performed.

Currently, operations are in progress to test the fuel-handling gripper on the fixed subassembly (welded in place) and to remove the two "fill filter" subassemblies (one in the core and one in the outer blanket) prior to operation of the primary pumps.

The fuel-unloading machine and its temporary argon cooling system are being tested in preparation for handling filter subassemblies.

In the process of operating the three reactor cover-locking mechanisms, one of the locks failed to raise to its full "up" position. Preliminary examination indicates that it is mechanically bound. Although this will not affect current operations, investigation and correction will be necessary before primary pump operations can start.

A small fire occurred during the early morning of March 27 and involved the vapor trap in the temporary cold-trap loop in the primary sodium system. A fire alarm was sounded, but the fire was extinguished by local action before the arrival of firemen a few minutes later. Damage was estimated at less than $25, and one person received slightly singed hair and minor skin irritation. The cause was the failure of a vent pipe which had developed a small hole in its wall.

2. Sodium Boiler Plant

The secondary sodium-storage tank was maintained at 350°F by means of electrical heaters. Circulation through the cold trap continued under isothermal conditions. Runs made on the 8th, 9th, and 10th of March showed plugging temperatures in the range from 280°F to 300°F, which is equivalent to a concentration of 8-10 ppm oxygen in the sodium. A distillation sample taken on the 10th showed 9.2 ppm oxygen.

A total of 55 drums (with a 55-gal capacity) were filled with sodium from the final tank car and are stored for future use. The yard sodium-unloading piping was dismantled and the tank cars readied for removal from the EBR-II area.

While cleaning the sodium tank car transfer piping, a plug of sodium was projected from a pipe assembly and landed on the top deck of the cooling tower. Since sodium is an excellent incendiary agent, immediate precautionary measures were taken by turning on the cooling tower water and sending in a fire alarm. Net damage consisted of a scorched area less than one foot square.

Additional thermocouples were added to the shells of the evaporators and superheaters to furnish a more complete temperature profile during initial filling of the steam generators and secondary-system piping. An argon gas sample was taken from the secondary sodium system to provide a reference standard for hydrogen concentration in the blanket gas. This could be useful in the future, as an increase in hydrogen content would indicate a possible leak and sodium-water reaction. The Ansul fire-protection system piping in the northeast corner of the boiler wing was accidentally briefly discharged, filling the pipe with powder (Met-L-X). The piping was disassembled, cleaned, and reassembled.

3. Power Plant

After reviewing the heat-up of the steam system to 350°F, certain design deficiencies and equipment malfunctions became apparent. Most of these were listed in the Progress Report for February 1963, ANL-6698, p. 17. The effort this month has been directed toward correction of these conditions. Work in the following areas has been completed:

Number 2 Deaerating Heater. The original spray headers were replaced with new spray headers of modified design to improve performance at low loads. The heater was opened up, cleaned, and the level of the trays verified.

Condensate Piping. New and revised lines were installed in the condensate system to provide added operational flexibility at low loads and to prevent the severe water hammer experienced during the initial heat-up.

Block and bypass valves were installed at the control valve in the condensate line which returns excess system water to the condensate storage tank.

Condensate Storage Tank. When this tank was opened for inspection, it was found that the vinyl lining had failed. The lining was removed, and it was decided not to replace it in this aluminum tank. To avoid excessive aeration of the water in the tank, dip pipes with suitable anti-siphon devices were installed for the makeup line and the excess condensate return line.

Yard Lines. The yard lines were surveyed and found to have pockets due to incorrect pitch. Since ice had formed in these lines, they were hydrostatically tested and found to be uninjured. The hangers will be adjusted at a later date to correct the pitch.

Condenser. The condenser was opened, inspected, and cleaned.

Miscellaneous. Duplex strainers were installed in the cooling water line leading to the gland exhauster pump and spray chambers on the turbine.

Remote drives were installed on some inaccessible valves.

The insulation damaged by the modifications was repaired and painting is underway.

Flow-metering orifices have been installed in the discharge lines downstream instead of upstream of the check valves as previously. These meters discharge from the circulating pumps and eliminate chattering of the check valves.

4. Fuel Cycle Facility

To fill the Argon Cell with argon gas, it is necessary to remove shielding plugs from the passages that are used for the filling operation. After the filling of the cell has been completed, it is necessary to reinstall the shielding plugs. While the plugs are being reinstalled, the Argon Cell is open to air. Investigations were undertaken to determine the effect that such exposures to air will have on the composition of the cell atmosphere. These studies were made while the cell was filled with nitrogen which had been introduced into the Argon Cell for the purpose of making air inleakage tests of the sealed cell (see Progress Report for February 1963, ANL-6698, p. 18). In the new series of tests, several penetrations in the Argon Cell were opened to air one at a time while the pressure in the cell was near atmospheric pressure. The cell penetrations were made for various periods of time (up to 5 min). The passages opened included a horizontal penetration in the wall (5 in. in diameter by 5 ft long), a vertical penetration in the cell (7 in. in diameter by 5 ft long), and both ends of one of the small transfer locks. The opening of these penetrations resulted in no marked change in

the oxygen level in the cell atmosphere. When both ends of the large (6-ft-diameter) transfer lock were opened for $4\frac{1}{2}$ min, the oxygen level in the Argon Cell increased from 10 ppm to approximately 300 ppm. During all the tests, there was no detectable increase in the inventory of gas in the Argon Cell.

A failure of a bearing in the compressor used in the argon purification system occurred toward the end of the air inleakage tests. The bearing was removed and is being studied to determine the cause of its failure. To remove the bearing, it was first necessary to remove the compressor from its enclosure. The removal of the compressor was difficult. To overcome this difficulty, the compressor enclosure is being redesigned.

A filter is being designed to remove oil which is entrained in the off-gas from the vacuum pumps for the melt-refining furnace. The filters will serve to prevent the entrained oil from reaching the activated carbon bed in the off-gas delay tank. The delay tank will be used to store the gases that are released in melt refining and in the oxidation step of the skull-reclamation process until meteorological conditions are favorable for the discharge of the gases through a 200-ft-high stack.

Two stereo-optical depth perceptors have been fabricated at Argonne for use in viewing remotely controlled manipulator operations through the shielding windows of the process cells of the Fuel Cycle Facility (see Progress Report for May 1962, ANL-6573, p. 22). The viewing qualities of the instruments are found to be excellent. Portable floor mounts for the units are being built.

Storage racks which will be capable of holding either four fuel subassemblies or four control subassemblies are being designed for use in two of the 12-in.-diameter storage pits in the floor of the Air Cell. Air (120 cu ft/min at 2 psi) for cooling the subassemblies will be provided by a lobe-type blower. The flow of air will be automatically controlled so that the flow rate will be nearly constant whether or not subassemblies are in the storage racks.

Since declad fuel pins from spent EBR-II fuel subassemblies may be stored in stainless steel storage vessels, two exploratory experiments were performed in a vacuum-type glove box to determine whether an alloying interaction occurred between the bare fuel pins and stainless steel (type 304) surfaces of the storage vessels. In the first experiment, no interaction was noted when polished fuel pins were heated at 550°C for three hours in contact with a stainless steel surface. In the second experiment, the polished fuel pins were first wetted with sodium and then placed in a stainless steel (type 304) box with a removable cover. Again, no interaction was noted between the fuel pins and the stainless steel surfaces of the box upon heating the pins at 450°C for two hours. It was noted, however, that all of the sodium had evaporated from the pins, and had deposited on the inside surface of the box cover.

Remote installation of the decanner was completed, and electrical and pneumatic checkouts were made. Reference thermocouples for the melt-refining furnace have been calibrated in place. Checkout of valve cabinets for injection casting, pin processing, and welding stations has been completed.

The air cell was utilized to remove the first several-thousand-curie antimony source for the EBR-II reactor from its irradiation capsule, and to attach it to suitable fixtures for handling in the reactor. Considerable cell contamination was encountered, which apparently arose from the presence of a loose, highly active deposit on the surface of the tantalum-clad source. Decontamination of the cell has been substantially completed.

Most of the hardware to permit making several hundred fuel assemblies has been obtained, except for fuel-element components and completion of grid castings. Difficulties have been encountered by vendors in meeting specifications for element tubing and end fittings. However, delivery of the first group of acceptable spades has been made, restrainers and tubing are expected shortly, and the initial phases for the production of complete cladding units are underway.

The analytical laboratory has put into routine use the Chemistry Division's technique for determining carbon in sodium. This involves measuring the volume of carbon dioxide produced after perchlorate oxidation. At the 40-ppm level, replicate analyses within ±10% were obtained on reactor samples. A spectrophotometric method for determining concentrations of rare earths as low as 0.01% in fissium alloys as their arsenazo complexes has been developed. Separation involves oxalate precipitation and trioctylphosphine oxide extraction.

5. Fuel Development

a. Fuel-jacket Development. In addition to continuing work on the four niobium-base alloys mentioned in the Progress Report for February 1963, ANL-6698, p. 20, annealing studies are in process on the EBR-II Core II reference alloy, Nb-1 w/o Zr. The properties of Nb-1 w/o Zr are dependent upon fabrication history, heat treatment, and level of interstitial elements. The studies consist of determining proper stress relieving and recrystallization temperatures for Nb-1 w/o Zr rod and tubing as a function of degree of deformation, type of deformation (i.e., swaging, drawing, and rolling), and level of interstitial-element contamination. Analysis will be based on hardness data and metallographic examination.

b. Uranium-Molybdenum Alloys. Radiographic inspection confirmed the apparent results of rolling tests reported in Progress Report for February 1963, ANL-6698, p. 21. Specimens which had received 6.5 and 19% total reduction were successfully rolled to about 82% at 1050°C to 1100°C, with 8-16% reduction per pass.

c. Postirradiation Examination of Reference EBR-II Core I Fuel Elements. Work is continuing on the examination of reference EBR-II Core I fuel elements which have been irradiated in NaK capsules in the MTR. The postirradiation density measurements of the jacketed elements indicated a slight increase in overall volume. This volume increase was equivalent to a uniform increase of diameter of less than 0.001 in. Radiographs of the jacketed fuel cores indicated that the U-5 w/o Fs alloy cores decreased in length. The U-5 w/o Fs-2.5 w/o Zr alloys showed a scatter in the data with some cores increasing in length, some decreasing, and some not changing at all.

Dejacketing of representative elements is now in progress. A comparison of the diameter, length, and volume changes based on density measurements for both the jacketed elements and fuel cores disassembled to date is given in Table IX. In general, there is an increase in diameter, decrease in length, and increase in volume. The measured diameter increases of the fuel pins are less than is required to completely fill the jacketed assembly. It appears that the jacketed EBR-II Core I fuel elements can be expected to increase slightly in diameter before the fuel core has expanded against the jacket.

Table IX Physical Changes on Irradiated Reference EBR-II Fuel Elements

Element No.	Composition,[a] w/o		Max Irradiation Fuel Temp, °C	Est Max Burnup, a/o	Volume Change of Jacketed Assembly, %	Fuel Core		
	Fs	Zr				Max Dia Change, %	Length Change, %	Volume Change, %
ET-3-14	5	-	640	2.2	0.43	4.9	-1.4	4.1
ET-1-8	5	-	500	1.8	0.25	2.8	-1.3	2.9
ET-2-2	5	2.5	600	1.5	0.26	4.2	-0.5	4.4

[a] Balance is uranium.

d. Properties of Uranium-Plutonium-Fissium. Bend-test specimens of the U-20 w/o Pu-10 w/o Fz and U-10 w/o Pu alloys have been injection cast and machined. Both alloys will be tested in the as-cast and heat-treated conditions. Bend testing of the U-10 w/o Pu-10 w/o Fz alloy showed that homogenized specimens, heat treated for stabilization of high-temperature phases, had twice the bend strength of as-cast specimens. Metallographic examination of the fractured specimens revealed that the fracture surface of as-cast specimens was not as coarse as the fracture surface of heat-treated specimens. Further metallographic studies are being made of these specimens

Bend testing of the U-10 w/o Pu-10 w/o Fz alloy included testing of notched specimens which had been prepared for the Hounsfield Impact Tester. The heat-treated specimens were found to have greater notch sensitivity than the as-cast specimens.

Table X shows the data obtained from a series of tests of the hot tensile properties of a U-10 w/o Pu alloy at various temperatures to 700°C. The tensile strength decreases with temperatures from 37,500 psi at room temperature to 8,280 psi at 700°C. Note that brittle failure occurs at all temperatures. We qualify the modulus data because uranium does not exhibit a linear portion on the stress-strain curve at any temperature. Our values are probably low, and the error greater as the temperature increases. The α-β phase transformation occurring at approximately 590°C is associated with discontinuities in the tensile data.

Table X. Elevated Temperature Tensile Properties of U-10 w/o Pu Alloy

Tensile Strength (psi ±1%)	Yield Strength (0.2% offset)	Modulus of Elasticity (10^6 psi)	Temperature (°C)	Remarks
37,500	-	19.1	23.5	Broke before yield strength could be established.
32,740	-	-	305.5	Broke before yield strength could be established.
23,200	21,080	8.16	454.0	
18,980	16,980	11.6	502.0	
13,320	13,280	14.4	550.0	
14,840	-	15.7	589.0	α-β transformation
9,600	-	7.38	651.0	Broke before yield strength could be established.
8,280	8,100	0.96	700.3	

We compared tensile data from EBR-II fuel pin size specimens with that of the $\frac{1}{4}$-in.-diameter specimens mentioned above. Premature fracturing in these pins, probably due to the microporosity, caused us to abandon their use.

(i) Kinetics of Transformation. The transformation kinetics of U-Pu-Fz alloys are being investigated to aid in the evaluation of the properties of these alloys. The U-10 w/o Pu and U-10 w/o Pu-10 w/o Fz alloys are being studied using hardness and metallography as tools.

Specimens of the alloy were made from EBR-II pins, cut to approximately $\frac{3}{8}$ in. long. These were homogenized for four days at 850°C and cooled. Each was then heated to 700°C, without encapsulation, for $\frac{1}{2}$ hr, and quenched in a lead bath, held at 450, 500, and 550°C for different times, and quenched to room temperature in oil.

The hardness changes indicate degrees of transformation. Complete transformation is indicated when hardness does not change with time. The results indicate that the complex transformations begin before 5 min at all three temperatures. The change in hardness varies for the different holding temperatures; the as-quenched value is 62 R_A. At 450°C, a maximum of approximately 74 R_A is reached in approximately 20 min, and at 500°C, 72 R_A in approximately 60 min. At 500°C a peak of about 65 R_A occurs in about 100 min. At all temperatures hardness peaks are followed by further changes, but at 1000 min they are not different by more than 1 R_A unit from the maximum.

(ii) Compatibility of Plutonium-bearing Fuels with Cladding Materials. U-Pu and U-Pu-Fz alloys are being tested for compatibility with potential refractory metal claddings to help in the selection of a fuel and cladding material for EBR-II, Mark II loading.

The fuel/clad combinations that are being studied are U-10 w/o Pu and U-20 w/o Pu-10 w/o Fz with Nb and U-10 w/o Pu-10 w/o Fz with Nb, Nb-1 Zr, Mo, and V. These combinations will be studied in the temperature range from 550 to 650°C by making diffusion couples and annealing them for 1, $2\frac{1}{2}$, and 6 weeks.

All these couples have been assembled and are being annealed. The short-time heat treatments have been completed and the specimens are being studied metallographically.

6. Process Development

a. Melt-refining Process Technology. A preliminary laboratory-scale experiment has been performed to determine the behavior of fission product cesium and iodine, which are volatilized in the melt-refining process. Unirradiated uranium-5 w/o fissium alloy to which inactive cesium metal and uranium iodide had been added was melt refined under argon for one hour at 1400°C. Both cesium and iodine were collected on a tantalum condenser above the crucible. Condensate and equipment components were analyzed, and distribution of the two elements were as follows (as percent of charge):

	Product Ingot	Crucible	Skull	Volatilized
Cesium	<2	52	5	27
Iodine	<0.5	-	<0.3	28

The low material balance for iodine may result from the inadequacy of the wet chemical method used in the analysis of the iodine in the crucible. The use of a radiochemical procedure for this analysis is being considered. Modification of the experimental equipment is also being considered in an effort to find the cause of the large iodine loss.

b. Skull-reclamation Process. Work was continued on the development of the skull-reclamation process for the recovery of skull material which remains in a zirconia crucible after melt refining. In an attempt to improve the capability of the process to remove zirconium, a process modification was incorporated into a demonstration run performed on a 130-g uranium scale. This consisted of adding iron to the uranium-zinc product solution obtained after the reduction step in an attempt to precipitate the zirconium from solution. The addition of iron effected an inadequate precipitation of zirconium (about 15 percent). In another demonstration run, carbon was added at the conclusion of the reduction step in an attempt to effect zirconium removal. Analyses of the material from the carbon run are not yet completed.

Process operations have been started in the recently completed skull-reclamation-process pilot plant (scale: $2\frac{1}{2}$ kg of skull oxide). Three runs were performed in which agitation of zinc and flux for several hours under noble metal-extraction conditions was followed by successful transfers of zinc from beneath solidified flux at 525°C. The percentages of zinc transferred ranged between 92 and 97 percent. Transfer of flux from the uranium-zinc phase at 800°C after the reduction step was achieved by manually controlled pressure siphoning, using a bubbler gauge to determine interface level. Both of these steps were carried out in a tungsten crucible (13-in. OD by 19 in. high) which appears not to have been affected by process operations to date.

The skull material remaining in the crucible after melt refining adheres to the crucible walls and cannot be easily removed. In previous runs of the skull-reclamation process, complete oxidation of the skull material resulted in a powder that was readily poured from the crucible (see Progress Report for February 1963, ANL-6698, p. 20). However, the use of partial oxidation rather than complete oxidation of the skull material to effect its removal from a melt-refining crucible has been suggested, since this method, if successful, would lead to a simplification of the oxidation process and of the required equipment (see Progress Report for January 1963, ANL-6683, p. 16).

Two runs were made to test this method. In these runs, the uranium-fissium-cerium skulls were partially (50 percent or less) oxidized in the skull-oxidation furnace. The two runs showed that partial oxidation resulted in powdering only a fraction of the skull material. The powdered material could be readily poured out of the crucible. The material remaining in the crucible, however, retained the cup shape of the original residue

from the melt refining step. Although this residual material was loosened from the interior surfaces of the crucible, the material could not be dumped by inverting the crucible.

Distillation equipment is being tested for the removal of residual magnesium-zinc from uranium in the last step of the skull-reclamation process. A new distillation unit, which can be used with the melt-refining furnace base has been previously described (see Progress Report for January 1963, ANL-6683, p. 16). This unit, which consists of a distillation crucible, a vented crucible cap, a disposable collector, and a condenser was used to make two additional distillation runs. In each run, 1000 g of 50 w/o magnesium-zinc was charged to the crucible. The distillations were carried out under reduced pressure (1 mm Hg). The major temperature arrest was at approximately 670°C. In the first run, all the magnesium-zinc was distilled from the crucible and was found to be distributed as follows: 90 percent in the collector, 6 percent in the condenser, and 4 percent in the annulus between the collector and the vented crucible cap. Although the collector and the vented crucible cap were bonded to each other, the condenser and collector, and the collector and the crucible cap could be easily disassembled from each other.

In the second run, a graphite felt seal washer was used to minimize the possibility of having distilled molten metal enter the annulus between the collector and the crucible cap. At the end of the run, all the distilled metal was found in the collector and the condenser; none was found in the annulus between the crucible cap and the collector. The apparatus was readily disassembled and no sticking of equipment components was encountered.

c. Blanket-processing Studies. The seventh of a series of 500-g-uranium blanket-process demonstration runs has been completed. This process involves dissolution at 800°C of the plutonium-bearing blanket material in a 12 to 14 w/o magnesium-zinc alloy, precipitation of uranium by addition of magnesium to a concentration of about 50 w/o to precipitate the uranium, cooling, and removal of the supernatant phase (the plutonium product solution), whose volume will be reduced by evaporation, if necessary, to a volume suitable for feeding into a future core cycle.

In the most recent run, a depleted uranium charge containing fission product elements at the expected process levels was lightly irradiated prior to processing in order to obtain information on fission product behavior. In order to determine the behavior of iodine, a charcoal trap was used in the exhaust line of the furnace and a nickel strip 16 in. long was located on the upper wall of the furnace chamber to collect samples of any iodine that deposited. Considerable iodine activity (about one-quarter of the total) was found condensed on the upper wall of the furnace chamber, but little iodine activity (about 0.1 percent of the total) was found in the furnace off gases (i.e., only a small amount was removed by a charcoal filter unit).

The bulk of the zirconium and tellurium activities were also lost; only small percentages were found with either the uranium or plutonium products. The mechanisms for their loss and for the large loss of iodine have not yet been determined. As expected, ruthenium largely accompanied uranium through the process, whereas rare earths, yttrium, and barium and strontium appeared predominantly in the plutonium product solution.

d. Plutonium-recovery Process. The distribution behavior of neptunium, curium, protactinium, and chromium between zinc-magnesium solution and molten magnesium chloride at 800°C was investigated. Neptunium and curium have been found to distribute to the metal phase as does plutonium (see Progress Report for April 1962, ANL-6565, p. 27). Each has a minimum distribution coefficient at about 10 w/o magnesium in the metal phase. Preliminary results indicate that protactinium also exhibits the same general behavior as plutonium, but that its distribution coefficients are lower by about an order of magnitude. The distribution behavior of chromium is of interest because chromium from the stainless steel cladding may be a contaminant in the second EBR-II core, which is expected to contain plutonium. Earlier work (see Progress Report for April 1962, ANL-6565, p. 26) had shown that the other cladding constituents, iron and nickel, are readily removed from the fuel under noble metal-extraction conditions. Preliminary data on chromium, based on gamma counting of 27.8-day chromium-51, show distribution coefficient values of about 0.025 at 10 w/o magnesium, 0.10 at 40 w/o magnesium, and widely scattered values above 50 w/o magnesium. The reason for the scattering in the magnesium-rich alloy has not been determined.

D. FARET

1. Model Fuel Element (Zoned-core Test Zone) for Out-of-pile Tests

Simulated fuel pellets of lava and a platinum tube heater were installed in a quartz tube (simulating the fuel-element cladding) to permit visual observation of the internal behavior of the model fuel element (see Progress Report for December 1962, ANL-6672, p. 22). The maximum heater temperature in this test was about 1460°C; this resulted in pellet surface temperatures of about 900°C (measured by optical pyrometer), a linear heat flux of about 21.4 w/cm [2230 Btu/(hr)(ft)], and a temperature variation through the pellets of at least 400°C. When the air in the quartz tube was replaced by helium through a $\frac{1}{8}$-in.-OD tube, 20 ft long, to simulate reactor installation, the heater temperature decreased approximately from 1260°C to 970°C while the linear heat flux remained constant at 13.3 w/cm. This demonstrated the possibility of changing fuel temperatures in the FARET zoned-core test zone without changing reactor power.

2. Sodium Removal

Fuel assemblies removed from FARET will be covered with a thin film of sodium. Removal of this film before disassembly and postirradiation examination of the fuel will be necessary.

The possibility of using a fused salt eutectic for removing the sodium adhering to fuel pins or fuel assemblies after they are removed from the reactor has been studied. A cluster of seven EBR-II-type, stainless steel-clad, dummy fuel pins were coated with sodium and then immersed in a 41% KCl-LiCl mixture at ~357°C. Upon removal from the salt bath, the pins were free of sodium, but were coated with a very thin film of the salt mixture. This coating can be removed, if necessary, by flushing with warm water. No corrosion effects due to the molten salt were observed. In the event that cladding failure is suspected, the salt film might be removed with steam to minimize any reaction with bond sodium remaining in the fuel pins.

3. Physics

A four-group cross-section set (denoted as 216) was constructed for a carbide system of 3000-liter volume from a sixteen-group set (denoted as 195) for the purpose of investigating sodium- and fuel-expansion coefficients in a two-dimensional configuration. The sixteen-group set was generated from the fundamental mode computation (ELMOE). The calculations of the sodium coefficient were made in the one-dimensional code with the use of equivalent spherical geometry and critical enrichments computed for cylindrical geometries with length-to-diameter (L/D) ratios of 1 and 0.25. The reactivity coefficients were compared for the RE-122 computations for each set and in turn these were compared with a PDQ (two-dimensional code) calculation based on the four-group set. The preliminary results are presented in Table XI.

Table XI. Comparison of Sodium and Fuel Temperature Coefficients for One-dimensional 16-group and 4-group Cross-section Set, and Two-dimensional Computations for a 3000-liter Core

Volume Fraction PuUC/Na/SS (volume)	Critical Plutonium Enrichment, a/o	L/D	Sodium-expansion Coefficient, $(\Delta k/\Delta T) \times 10^6$			Fuel-expansion Coefficient, $(\Delta k/\Delta T) \times 10^6$		
			Set 195 (16-gp)	Set 216 (4-gp)	PDQ (4-gp)	Set 195 (16-gp)	Set 216 (4-gp)	PDQ (4-gp)
25/59/16	11.419	1	+4.4	+4.5	+5.2	-3.4	-3.33	-3.78
	13.168	1/4	+0.4	+1.44	+2.14	-0.9	-0.7	-2.22

The four-group set was found to lead to greater reactivity than obtained from the sixteen-group set. However, the reactivity coefficients for the system having L/D = 1 agreed for the two sets so that the one-dimensional method of computation appears to be adequate for this case. The discrepancy in the sodium-expansion coefficients between the two sets for the L/D = 0.25 geometry is unsatisfactory, although the four-group set gives fair agreement with the two-dimensional computation (PDQ). A new four-group set is being generated to get better agreement with the sixteen-group set. This again will be compared with the two-dimensional computations.

Two-dimensional computations were also carried out for the sodium coefficient in which sodium loss occurred only in the reactor core. This was compared with a similar computation in which the sodium loss occurred in the upper and lower blankets as well as in the reactor core. The upper and lower blankets were assumed to have the same composition as the reactor core except that the plutonium-uranium carbide was replaced with depleted uranium. The results are presented in Table XII. As expected, the sodium coefficient became more negative. A marked change occurred in the L/D = 0.25 geometry.

Table XII. Sodium Coefficients for a Two-dimensional Computation (PDQ) for a 3000-liter Core

Volume Fraction PuUC/Na/SS (volume)	Critical Plutonium Enrichment, a/o	L/D	Sodium-expansion Coefficient, $(\Delta k/\Delta T) \times 10^6$	
			Reactor Core	Reactor Core and Upper and Lower Blankets
25/59/16	11.419	1	+5.2	+4.2
	13.168	1/4	+2.14	-3.74

The preliminary results indicate that the outer region of a system in which there is a leakage component contributes an appreciable negative effect for reactivity coefficients.

4. Development of Ceramic Fuels.

During the past month work continued on the development of a UO_2 extrusion proposed by the fuel design for FARET. Much difficulty had been encountered in achieving a sound body as a result of warpage and excessive cracking. However, by adjusting the binder content, sound rods have been extruded.

III. GENERAL REACTOR TECHNOLOGY

A. Applied Nuclear Physics

1. Recoil Counter for Fast-neutron Spectroscopy

The small recoil counter designed for making in-pile measurements of fast-neutron spectra has been assembled and satisfactorily tested, although some essential calibration measurements are yet to be made.

In order to arrive at an optimum gas for recoil counter work, tests were run with counters containing various relative amounts of hydrogen and methane (with ~1% by volume of N_2 to supply a calibration proton line). Pure hydrogen counters are subject to "ultraviolet" instabilities in which photons are liberated near the anode during the avalanche and cause photoelectrons to be ejected from the cathode. The addition of a quenching gas, such as methane, will absorb ultraviolet light and stabilize the counter. Stable operation, as evidenced by an exponential increase of gain with voltage, was achieved with about 10% by volume of methane in hydrogen.

This mixture is probably near optimum for recoil work of high gas multiplication. It is better than pure methane because carbon recoils are smaller, as are nonlinear energy-ionization effects.

Some spectra were measured with the counter by subjecting it to mixed gamma-neutron fluxes. Gammas commence to appear significantly at 50 kev and fall off at lower energies. Rate-of-rise spectra can distinguish between proton recoils and electrons as low as 300 ev; no attempt was made to record events of lower energy.

Observations at a few hundred electron volts revealed some electronic problems. When gas amplification is sufficient to observe rate-of-rise spectra at 300 ev, events corresponding to proton recoil near 1 Mev (which is the upper limit at 1 atm gas pressure) severely shock the simple amplifiers currently being used. Recovery is not very rapid and distortion may result.

It is probably not worthwhile to investigate below 300 ev since the requirement of about 30 ev per ion pair introduces a very large variance in the results (~50%).

Current work is directed towards developing more complete understanding of the probe and its limitations. A two-parameter multichannel analyzer will probably be used with the probe since the gamma rejection gate in the present system has to be set and calibrated to very exacting limits. The value of an analyzer is that it will do routinely what presently must be done with complex and somewhat personalized apparatus.

2. High-conversion Critical Experiment (ZPR-VII)

The 1.24-cm square pitch pattern of the 3% enriched, stainless steel clad was restored and some of the earlier measurements reported last month (Monthly Progress Report for February 1963, ANL-6698, p. 33) were repeated. This was done to obtain a more accurate determination of certain intercell parameters. These measurements are essentially complete and most of the experimental data have been processed.

The U^{238}-to-U^{235} fission ratio, δ^{28}, has been determined in this 1.24-cm square stainless steel Hi-C core. The hydrogen-to-U^{238} atom ratio for this lattice was 2.93. The quantity δ^{28} was measured by irradiating enriched (3.23 w/o) and depleted (0.21 w/o) uranium-metal foils in axially symmetric positions in slotted fuel pins. Three such pins were irradiated in each of two reactor runs, giving 18 values of δ^{28}. The resulting mean and the standard deviation was $\delta^{28} = 0.0984 \pm 0.0046$. Using values of $\nu^{25} = 2.43$ and $\nu^{28} = 2.84$, one obtains for the fast fission factor $\epsilon = 1.075 \pm 0.0035$.

The disadvantage factor A for the 1.24-cm square stainless steel Hi-C lattice was also redetermined. The U^{235}-fission-cadmium ratio in the fuel was determined with an accuracy of about 2%, whereas the U^{235}-fission-cadmium ratio in the moderator could only be determined with an accuracy of about 6%. This error was primarily due to uncertainties in the position of the foils when sampling a representative portion of the moderator cross section. With these errors a disadvantage factor of $A = 1.23 \pm 0.056$ was obtained. When a nonrepresentative (that is, does not conform to moderator cross section) cadmium-covered moderator foil was used, the disadvantage factor was found to be $A = 1.26 \pm 0.057$.

This would indicate that, for this type of measurement in a tight lattice, the cadmium-covered foils do not have to be matched in shape to the cross section of the moderator. Using average cross sections obtained from the results of SOFOCATE problems, one obtains for the thermal utilization in this lattice $f = 0.849 \pm 0.010$.

The analysis of the buckling measurements made in the uniform 1.24-cm square stainless steel Hi-C core (see Table XIII) has not been

Table XIII. Analysis of Buckling Measurements in the 1.24-cm sq Hi-C Lattice

Number of Determinations	Type of Foil	$\overline{R}$, cm	B_R^2 [10^{-3}], cm^{-2}	λ_R, cm
12	bare	37.77 ± 0.357	4.598 ± 0.076	8.648 ± 0.357
8	cadmium	36.80 ± 0.340	4.815 ± 0.079	7.632 ± 0.340

completed. There exists about a 1-cm difference in the extrapolated radius between results obtained from bare-foil measurements and those obtained from cadmium-covered-foil measurements. The errors quoted are standard deviations from the mean. The data were fitted out to a radius of 24.8 cm. The criterion used to define the extent of the radial asymptotic region, or the distance beyond which no points would be used for fitting, was a gold-cadmium ratio independent of radius. The above data suggest that new criteria are needed.

Two additional fittings of the same data are now being done out to radii of 19.8 cm and 14.8 cm. It is hoped then to find the fitting radius for which the bare and cadmium-covered B_R's are identical and independent of radius.

The value of the resonance escape probability p_{28} calculated from experimental data is $p_{28} = 0.685 \pm 5\%$ for the 1.24-cm square lattice; here, the quoted error is the fractional standard deviation. The basic experimental quantity used in this determination is ρ_{28}, defined by

$$\rho_{28} = (U^{238} \text{ Capture Cadmium Ratio} - 1)^{-1} \quad .$$

The measured value for ρ_{28} is $3.72 \pm 14\%$.

A tentative value of 0.55 has been obtained for the initial conversion ratio (ICR) in this Hi-C, 3 w/o enriched stainless steel, 1.24-cm square lattice core. Bengston and Hellens[3] give a theoretical value of the ICR of about 0.52 for an $H:U^{238}$ atom ratio of ~3 and an uranium enrichment of 3 w/o. A second run has been made in order to increase the precision of the value, and data are now being obtained from these foils. Information is also being obtained from the rerun regarding the dependence of the fission product correction (that made from the Np gamma coincidence count rate) on spectrum. Foils of very highly depleted uranium (6 ppm other than U^{238} atoms) were also irradiated to ascertain the effect, if any, on the enrichment of the detector foils.

3. Measurements of Flux Perturbation

Progress in the systematic study of the internal and external changes in the neutron-flux distribution pattern caused by the introduction of an absorbing material into a moderating medium was last reported in ANL-6580 (Progress Report for June 1962, pp. 31-32). Plans to continue and expand the program by utilizing the higher levels of neutron flux available at the JUGGERNAUT reactor were mentioned then. Soon thereafter, foil activations at

[3] J. Bengston and R. L. Hellens, A Survey of the Beginning of Life Characteristics of Uranium-fueled, Water-moderated Lattices, CEND-137.

ATSR were suspended and attention directed to the construction of appropriate experimental facilities at the JUGGERNAUT facility. The last measurements were made with parallel bare foils held vertically to the reactor face in the cadmium-lined void. The results of the measurements agreed essentially with those made in the same geometry with aluminum-covered foils. These experiments thus eliminated the suspicion that in some geometries even aluminum covers can make a serious difference.

The southern test cave of JUGGERNAUT was filled with graphite, and converted into a thermal column in which the foil experiments could be continued. In addition to repeating and extending the flux-perturbation measurements started last spring in the ATSR, a program was started to irradiate spherical probes (of ~1-cm diameter) and scan the activation of the surface by counting soft gamma or beta radiation. Experiments of this type should yield information about angular flux distribution. Although a spherical probe considerably reduces the total flux, the angular distribution is distorted only as a second-order effect.

The experimental equipment required to make the first measurements is now installed in the JUGGERNAUT facility. The central part is the 20 x 20 x 20-cm aluminum box which had previously been used in the ATSR. This box is lined with cadmium on five sides; the side facing the core of the reactor is open. It is located in the outer part of the graphite column of the facility. It is possible to insert foils into its interior (which is void) through one of the vertical access holes and an opening in the box cover. The open face of the box produces a known flux anisotropy at the foil location at its center.

Irradiation of a standard gold foil indicated that the flux level at the facility is about 10^9 n/(cm^2)(sec), as expected. A radiation survey at the access hole confirmed that it will be possible to exchange foils while the reactor is operating.

The current program will repeat in somewhat more detail the flux-depression experiments. In addition, gold spheres will be irradiated in the box and then surface counted. The activation over the surface of the sphere should give a quite good indication of the angular flux distribution, especially after the outermost gold layer of about 0.5 mm is removed by either mechanical or chemical means. This outer layer contains most of the activity caused by resonance neutrons and by those neutrons having entered the surface under a small angle. Suitable counting facilities for both foils and spheres have been assembled.

4. Sodium Absorption as a Spectral Index

The equipment developed to make absolute determinations of neutron-absorption rates by coincidence counting, as described in ANL-6683 (Progress Report for January 1963, p. 24), is now being used to study neutron

spectra in certain zoned critical assemblies in ZPR-III. It has been proposed that the ratio of neutron absorption at the 3-kev resonance in sodium to the U^{235} fission rate might provide a sensitive indicator of minor spectrum changes in dilute fast reactor assemblies.

Radiochemical techniques are now used routinely for making absolute fission-rate determinations. Currently, the sensitivity achievable in the detection of sodium activated in the ZPR-III is being investigated in order to estimate the precision possible in a determination of spectral change.

Several preliminary experiments were undertaken to determine the highest possible counting efficiency per gram of sodium with a beta-gamma coincidence system. It might be noted that gamma-gamma counting with sodium is also feasible, but it is inherently more difficult to achieve the same accuracy possible with beta-gamma detection.

Using $NaNO_3$, it was observed that about 0.3 gm may be incorporated in a liquid scintillator and still be counted with 96% (beta) efficiency, which is sufficient for absolute counting. More interestingly, a 25% efficiency was obtained by detection of Cerenkov radiation for as much as 7 gm of $NaNO_3$ dissolved in distilled water and placed in the counting vial.

The first sample received had an initial count rate of about 500 disintegrations/sec in 3 gm of powder; thus, it was necessary to do Cerenkov counting for the entire amount in order to maximize the gamma channel signal-to-background ratio. This low beta-channel efficiency necessitates a secondary calibration with samples of high specific activity; this is being done with a Cerenkov sample, a high-efficiency liquid scintillator sample, and by 4π beta counting by the radiochemistry group. The data are being processed by the computer program for coincidence counting, adapted for these special conditions.

It is a noteworthy conclusion that a surprising number of isotopes may be counted in a relatively high-efficiency mode by dissolving a rather large quantity of a suitable chemical form in water for Cerenkov counting. Since sample preparation is simple and quite accurate, it leads to many potential uses in cases for which large samples must be irradiated in order to obtain sufficient activity. One extension of these observations was tested with Co^{60}. The beta-end-point here is 0.3 Mev; the Cerenkov threshold in water is 0.17 Mev; accordingly, there is only a small contribution from betas, but the counting efficiency approached 10%. This is attributed to production of Compton electrons and subsequent detection of photon radiation. Thus, there is now available a useful Compton detector of gamma radiation.

5. Theoretical Physics

a. Mathematical Numerical Methods Analysis. A variety of efficient methods are available for constructing polynomials which take on specified values at n specified base points. If more general types of interpolating functions are required, the selection of techniques is far more limited. To assist in exploring the properties of the large class of interpolating functions which may be considered as linear combinations of a linearly independent set of basic functions, an inductive scheme has been constructed as follows: Let $\delta_i(x)$ be any function which vanishes at the base points x_j for $1 \leq j \leq i$, and which does not vanish at x_{i+1}. (The functions being treated may depend on one or several independent variables.) Let $P_i(x)$ be a function which takes on specified values, f_j, for $x = x_j (1 \leq j \leq i)$. Then, setting $P_0(x) = 0$, the recurrence relation

$$P_{i+1}(x) = P_i(x) + a_{i+1}\ \delta_i(x) \quad ,$$

with

$$a_{i+1} = [f_{i+1} - P_i(x_{i+1})]/\delta_i\ (x_{i+1}) \quad ,$$

will generate interpolating functions P_i which are linear combinations of the δ_i and which interpolate to the desired values for all $j \leq i$.

In the case of functions of a single independent variable, if we generate the $\delta_i(x)$ by the recurrence relation $\delta_0(x) = 1$; $\delta_i(x) = (x - x_i)\ \delta_{i-1}(x)$, the resulting interpolation function is a polynomial in x, and the algorithm is identical with the divided difference algorithm. If $\delta_0(x) = 1$, $\delta_i(x) = \sin\ (x-x_i)\ \delta_{i-1}(x)$, we generate trigonometric interpolating polynomials, and so on.

The variety of types of interpolating function which may be generated, the ease of programming the technique for a digital computer, and the insight which this approach gives into the interpolation process all contribute to its interest.

b. Reactor Physics Data Analysis ZPR-VII. Escape probabilities for neutrons born uniformly and isotropically in a fuel element were calculated by means of various approximations for both slab and cylindrical lattices. Calculations were made for a range of fuel-element transparencies and spacings.

For slabs, the methods used were (1) the exact formula, (2) the exact formula for an isolated slab with the mean chord length in the fuel divided by 1-C where C is the Dancoff factor, (3) the Wigner rational

approximation[4] modified as in (2), and (4) the Nordheim approximation.[5] For some cases, method (2) gave results in closer agreement with method (1), whereas for other cases method (4) gave better results.

For cylinders, three methods corresponded to methods (2), (3), and (4) above for slabs, whereas method (5) was used with the Fortran code 1692/RE (Progress Report for January 1963, ANL-6683, p. 25). Method (1) refers to Monte Carlo calculations reported by Rothenstein.[6] Methods (4) and (5) gave best agreement with method (1), whereas method (2) was also good except for quite transparent fuel rods.

The Fortran codes written last summer to calculate cadmium cutoff values are being revised to conform to the 704 monitor system, and various features are being added. As originally written, the codes calculate the cutoff energy for a 1/v-absorbing foil of arbitrary thickness between cadmium covers of arbitrary thickness in plane geometry for either an isotropic or a beam flux. The energy dependence of the flux was either a Maxwellian plus a 1/E tail, or the flux could be read in for a sufficient number of energy values. The revised codes will have the following changes. (1) Both cover and absorber foils have absorption cross sections consisting of a 1/v part and/or up to 100 Breit-Wigner resonances. (2) For the cases using a flux of analytical form, various options besides a sharply cutoff 1/E tail are available for the epithermal component. (3) Absorptions above and below the cutoff energy are calculated for both the bare and covered absorbing foil, and, in the analytical flux cases, for both the Maxwellian and epithermal components. (4) A printout of various functions for each point of the energy integration is optional.

B. Reactor Fuels and Materials Development

1. Ceramic Fuels

a. Plutonium and Plutonium-Uranium Carbides. Densities of sintered pellets of PuC were measured by the displacement method in bromobenzene liquid and found to be about 5% greater than the density values calculated from the dimensions and weights of the pellets. There are two ways to account for this discrepancy. The first is that the pellets may

---

[4] L. Dresner, Resonance Absorption in Nuclear Reactors, Pergamon Press, New York (1960), p. 60, Eq. (13-4).

[5] L. W. Nordheim, "The Theory of Resonance Absorption," Proceedings of Symposia in Applied Mathematics, Vol. XI, Nuclear Reactor Theory, pp. 58-88 (1961), Eq. (7.10).

[6] W. Rothenstein, Collision Probabilities and Resonance Integrals for Lattices, BNL-563 (T-151)(June, 1959); Nuc. Sci. Eng. 7, No. 2, 162 (Feb 1960).

contain 5% open porosity, which is not measured in the displacement method because the liquid penetrates the pellet and fills these voids. The second is to assume that the dimensions of the pellets, which are not perfect right cylinders, are in error by 5%. To determine which of these two explanations is correct an apparatus for accurately measuring the volume of pellets using a mercury pycnometer is being built.

The theoretical densities of the carbide compositions sintered at 1400°C are not accurately known because the compositions contain two phases and the phase boundaries of the Pu-C sinter have not been determined at this temperature. Since the percent of the theoretical density of a pellet is the only indication of the effectiveness of a sintering process and the theoretical density of carbides sintered at high temperatures could only be determined by a phase study, some other method of relating the densities or determining the amount of voids is needed. Present plans are to use lineal analysis on photomicrographs of the pellets to determine their percentage of voids.

Recent results of chemical analyses of the sintered pellets confirmed earlier data which showed that sintering at 1400°C for 2 hr does not cause the carbon content in the center to change from the value found in the arc-melted button before pulverization.

b. Corrosion Resistance of Urania Containing Burnable Poisons. The resistance of hydrogen-sintered urania-rare earth oxide compacts to corrosion by high-temperature, high-pressure water was studied. Samples which had been sintered at a peak temperature of 1700°C for 4 hr were exposed to 360°C water at a pressure of 2750 psi. Test times of 15, 69, and 138 hr in deoxidized distilled water and of 138 hr in oxygenated distilled water have been employed.

After 15 hr in deoxidized water, each of the rare earth-containing compacts had a small weight gain, while the 100% UO_2 sample had an appreciable weight loss. The physical appearance of the 97 w/o UO_2-3 w/o Gd_2O_3, 97 w/o UO_2-3 w/o Dy_2O_3, and 97 w/o UO_2-3 w/o Sm_2O_3 samples was changed only by the presence of a slight green corrosion product on the surface. The 97 w/o UO_2-3 w/o Eu_2O_3 sample had a thin, tightly adherent scale of green material, while the 100 w/o UO_2 sample had rounded edges and was covered with a readily removed, green powder. Under microscopic examination, the green corrosion product appeared as individual crystals which held tenaciously to the surface of the rare earth-containing samples.

There was little change in the appearance of the rare earth-containing samples after exposures of 69 and 138 hr in deoxidized water. The urania sample deteriorated markedly as exposure times increased.

The greatest damage to the samples was caused by a 138-hr exposure to oxygenated water. The compacts containing dysprosia and gadolinia were covered by a tightly adherent scale; the compacts containing samaria and europia had a frangible scale; the urania sample was covered with a green, dusting layer. Extreme weight losses occurred in the urania sample. Work is in progress to evaluate the compacts exposed in the oxygenated water for 15 and 69 hr to study shorter corrosion times.

Studies of the reactions which occur in unreacted mixtures of CeO, Eu_2O_3, Gd_2O_3, Sm_2O_3, and Dy_2O_3 with UO_2 are being made with the differential thermal analysis equipment.

c. Uranium-Thorium Sulfide. Uranium monosulfide was synthesized directly from uranium and sulfur by heating a pelletized mixture of powders having a sulfur-to-uranium ratio of 0.99 in a sealed argon-filled "bomb" container at 600°C for 45 min. The product consisted of a gray metallic clinker and a very small amount of loose black powder. Metallographic examination showed that the clinker was the monosulfide phase containing about 2% free uranium at the grain boundaries. Oxygen-bearing phases were found in a thin surface layer only. The black powder proved to be a mixture of US, γUS_2, and UOS. The clinker had a somewhat contracted lattice parameter of 5.4824 Å, indicative of foreign anions going into sulfur-lattice vacancies.

Further progress was made towards producing denser sintered US bodies free of the undesirable UOS and UO_2 phases. Compacts of US containing 0, 1, 2, 3, 4, 5, 7, and 9 m/o carbon were given a three-step firing treatment; (1) to 1600°C for 3 hr in vacuum to allow the carbon to reduce the UOS and UO_2 to US and UC, then (2) to 1825°C in vacuum for one hour to seal off the pellet surfaces, and (3) a switch to an argon atmosphere at 1825°C for the final 3 hr of sintering. The pellet containing no carbon sintered to 92% theoretical density, and a polished section showed very little UOS phase present. With 1 m/o C present, the amount of UOS was drastically reduced, and at 2 m/o C and above no oxygen-bearing phases could be observed. The density dropped steadily with increasing carbon content, but at 2 m/o C it was still 88% of theoretical. Measurements of lattice parameters generally substantiated the metallographic observations. They showed no change in the parameter of 5.4870 Å from 0 to 1 m/o C, a sharp drop to 5.4825 Å at 2 m/o C, and then a more gradual decrease to 5.4764 Å at 9 m/o C. The US-UC work showed a value of a_0 of 5.4764 Å occurred for a solid solution containing about 3 w/o UC. The parameters thus indicate that from 1 to 2 m/o C was needed to reduce the UOS or UO_2 present and that the excess carbon did reduce the US down to, but not below, its lower limit of homogeneity, which is believed to come at a sulfur-to-uranium ratio of about 0.96. Some free carbon was observed in the pellets containing 4 m/o and more C additions.

d. Uranium, Thorium, Plutonium Phosphides. The objectives of this study are to characterize the compounds in the different phosphide systems and to evaluate their potential as reactor fuel materials. Compounds are being synthesized by reaction of the solid elements and by reaction of uranium with phosphine gas.

Evaluation of the clinkers resulting from the direct reaction of the solids reveals that the high temperatures reached during the formation of the compound cause partial dissociation of the UP formed. X-ray diffraction shows a slightly smaller unit cell, which is believed to correspond to a substoichiometric composition (UP_{1-x}). Dissociation was aided when the reaction was carried out in an evacuated chamber. However, dissociation of UP has been virtually eliminated by use of a stainless steel autoclave. The combined pressure of the inert gas and the phosphorus in the autoclave suppressed the dissociation.

Nevertheless, the direct reaction method possesses two major drawbacks which outweigh the advantage of forming uranium monophosphide in one step. First, the high heat of formation limits the size of sample batches. Even more serious is the great difficulty in obtaining high-purity material. Finely divided uranium is an excellent oxygen "getter," and analysis shows that the powder picks up about 0.5% oxygen from the glove-box atmosphere. By indirect methods it has been determined that the high-purity red amorphous phosphorus used contributed about 0.6% of oxygen. Thus, the best UP made by this method contains about 1.1% oxygen, corresponding to about 9.0% UO_2.

Uranium monophosphide can be readily arc-melted. However, at these temperatures it exhibits considerable weight loss; after 4-min treatment, UP suffered a 7% weight loss. Part of the loss was due to congruent vaporization and part to dissociation into uranium and phosphorus. Uranium lines were detected in the X-ray photos of arc-melted material, and substantial amounts of phosphorus condensed on the cooler portions of the apparatus.

Synthesis of uranium phosphide has been carried out with phosphine gas (PH_3) as the phosphorus source. Synthesis was done in the gas train apparatus used to produce uranium sulfides. The compound U_3P_4 was formed at the reaction temperature employed, but it readily reacted with the free uranium present and/or decomposed at 1400°C to form UP. Relatively high-purity material was produced by this method, since X-ray reflections for UO_2 were barely visible, indicating a UO_2 content of 2% or lower (and an oxygen content of 0.2% or less). This is the UP of highest purity produced thus far.

X-ray analysis of this material showed a lattice constant of 5.590 ± 0.005 Å, corresponding to a theoretical density of 10.23 g/cc.

e. Thermal Diffusivity of UO_2. There is a need for detailed and accurate high-temperature thermal-conductivity data for sintered uranium dioxide bodies, especially above 1600°C, as well as for other sintered ceramic fuel. A series of transient experiments in TREAT has been performed, and results analyzed to test the feasibility of a transient experiment proposed for in-pile measurement of thermal diffusivity D (see Progress Report for June, 1962, ANL-6580, p. 54), where diffusivity D is related to the thermal conductivity k by the equation, $D = k/\rho C$, in which C is the specific heat and ρ the density of the ceramic. Briefly, the arrangement consists of two UO_2 cylinders, of the same diameter but different enrichments, which are joined forming one composite cylinder. Each half-cylinder contains a thermocouple located on the axis at a distance L from the interface of the half-cylinders. The composite sample is exposed to a transient reactor power burst, and the difference in temperature, ΔT, is measured at the two thermocouple positions. For given difference in enrichments, the true ΔT can be calculated as a function of time and diffusivity.

Two samples were used for the trial series and had enrichments of 10% and 11%, respectively, a diameter of 1.27 cm, and a length of 0.625 cm. Thoria-insulated tungsten-5% rhenium vs tungsten-26% rhenium thermocouples were used to measure temperatures. Nine transients with maximum sample temperatures ranging from 1450°C to 2250°C were performed. The thermocouple response was just barely adequate for use with unshielded specimens up to about 1900°C. At higher temperatures the thermal radiation from the sample became excessive and did not permit the ΔT value to be measured properly. At 2050°C, the time required to measure ΔT is overlapped by the time-response characteristics of the thermocouple. Analyses of data and photography indicate that the first transient on each sample provides the most reliable results, since cracking usually occurs at this time. From the experiments, the thermal conductivity was computed to be 0.026 (w)(cm)/°C and 0.038 (w)(cm)/°C at 1450°C and 1650°C, respectively. Re-evaluation of the data resulted in raising the 1450°C point to 0.030 (w)(cm)/°C. These values are consistent with published data.

Results are being evaluated to determine possible improvements, including yield of more than one experimental point from each sample, and extension of the technique to other temperature ranges and fuel materials.

2. Corrosion Studies

a. Zirconium Alloys for Superheated Steam.

(i) Flowing Steam. The flowing-steam tests referred to in ANL-6698 (Progress Report for February 1963, p. 40) have continued. During 28 days in 650°C, 600 psi, deoxygenated steam, the behavior of the Ni-Fe and Cu-Fe ternary alloys was similar to that in static tests. Flow rates were 100, 200, and 300 ft/sec. This test has been terminated, and new samples of the same alloys have been prepared for a test with oxygenated steam.

(ii) Hydrogen-pickup Experiment. It was reported previously that the above alloys absorb a far larger percentage of corrosion product hydrogen at 540°C than at 650°C. Recently, samples previously corroded at 540°C, which had absorbed about 1000 ppm of hydrogen, were exposed to 650°C steam for one month and then analyzed for hydrogen. The hydrogen content did not decrease. An increase was observed, which corresponded to only a moderate percentage of the new hydrogen produced by additional corrosion at 650°C. This is interpreted as evidence that the alloy hydrogen content is more directly related to the corrosion process than to some hydrogen equilibrium which may exist at the conditions of exposure.

(iii) Oxygen Absorption. Interest in oxygen absorption by corroding zirconium has been discussed previously. Recent analytical results show that the oxygen level in the Ni-Fe alloy increased from 1500 ppm after hot rolling to about 2200 ppm after 300 days in 540°C, 600 psi steam. The Cu-Fe alloy oxygen content remained at 1600 ppm during the same test. The distribution of oxygen within samples is rather uniform except perhaps for a thin layer near the corroded surface, where microhardness data and microscope appearance suggest a higher concentration of oxygen. At present the microhardness and microstructure data are available only for the Cu-Fe alloy.

(iv) Corrosion Film Studies. Metallographic studies of corrosion films produced by exposure to steam at 540°C for 300 days are being made. Cross-sectional micrographs at about 200X are being obtained of the film, interface, and underlying metal. Vertical cracks and transverse voids are prominent in the film. Description of the corrosion mechanism in terms of rate control at the interface rather than in the gross film is being considered.

b. Miscellaneous Materials in Water and Steam. Corrosion tests of TD nickel are being continued. Bar stock and sheet samples of TD nickel are being compared with "A" nickel in degassed water at 360°C and in oxygenated steam at 650°C and 600 psi. The material designated as "A" nickel was obtained from Argonne stock, and its history is not well known.

In the water test, wet-ground bar stock samples have been exposed for 50 days. Both the TD and stock nickel materials gained only about 0.28 mg/cm^2, but a portion of the corrosion product in each case was nonadherent and is not included in this figure. The TD material developed a few small blisters. (In steam testing, similar blisters appear to be associated with the particular sample rather than to be typical of TD nickel.)

In steam tests the bar stock TD material developed many small blisters (described in previous reports), while the reference bar stock "A" nickel formed a smooth adherent film. Table XIV shows the weight gain behavior of the two materials. Although the weight gains of the TD nickel were somewhat lower, its rate of gain was higher than that of the "A" nickel, which appears to have leveled off.

Table XIV. Corrosion of Bar Nickel in Oxygenated Steam at 650°C and 600 psi

Cumulative Exposure Time (days)	Cumulative Weight Gain, (mg/cm^2)	
	TD Ni	"A" Ni
17	0.69	1.69
26	0.98	1.65

In similar steam tests of rolled sheet stocks of TD nickel and "A" nickel, the weight gain behavior was similar to the above (see Table XV). Smooth, adherent films were formed on both materials, without the numerous, small blisters noted in tests of bar stock. However, the "A" nickel developed moderately large, swollen areas - perhaps from internal gas pockets - whose surface appearance was not unlike that of the rest of the sample. The behavior of pickled samples was similar, and the swelling phenomenon was again observed in "A" nickel.

Table XV. Corrosion of Sheet Nickel in Oxygenated Steam at 650°C and 600 psi

Cumulative Exposure Time (days)	Cumulative Weight Gain, (mg/cm^2)	
	TD Ni	"A" Ni
9.7	0.49	2.50
18.7	0.76	2.76
25.7	0.91	

c. Lightweight Alloy for Use with Mercury. Work on the use of inhibitors to reduce corrosion in liquid metal systems has continued. These studies are of general theoretical interest and may also result in relatively flexible conditions of operations, i.e. more than one additive may be suitable as an inhibitor.

As previously reported, the addition of zirconium to mercury considerably reduces the attack on titanium at temperatures up to 538°C under static conditions. Recent tests have indicated that the corrosion of titanium can also be reduced by the addition of nickel to the mercury. Duplicate specimens tested in saturated nickel solutions at 538°C showed a uniform protective layer. No significant weight change occurred after 14 days of exposure.

Studies are under way to identify the nature of the layer observed on the surface of these specimens. The layer appears as a continuous single phase, 0.37 mil thick. No transition or diffusion zone has been observed between the layer and the base metal. Spectrographic analysis indicates that this layer is primarily composed of nickel and titanium along with a small amount of mercury. Efforts to identify the compound by X-ray diffraction technique were not successful.

3. Nondestructive Testing

a. Ultrasonic Imaging. Life test studies on the first two sealed 2-in. ultrasonic pickup tubes are still in progress. Both tubes have been exposed to medium intensity ultrasound for several hundred hours, and no difficulty with the vacuum seal has been experienced. The last several sealed-off tubes have shown a tendency to gas during life test. However, recent tests indicate that this gassing has been caused by a modification of a metal part near the piezoelectric target which was not sufficiently outgassed during tube processing. Further tests to verify this are now in progress.

b. Correlation of Heat Transfer Properties and Bond Quality. The testing machines which are available to evaluate the strength of bonds give a shear test (e.g., the strength parallel to the plane of the bond) which is not as significant for bond quality as is a tension test. A modification of the ASTM:C97-55 apparatus can be made using existing equipment to provide a tension test on bonded specimens as small as 1 in.^{2}. It will also allow the specimens to be cut into bonded and defect areas, and allow the testing of these areas rather than the specimen as a whole.

c. Development of Instruments and Transducers. A lead zirconate titanate transducer (Clevite PZT-4 crystal) with an external ground was evaluated at the BORAX-V plate-testing facility. A depleted BORAX-V

superheater plate with artificial defects served as the test specimen. The results of this test confirmed earlier suspicion that such a ground would be unsuitable for dynamic testing. Consequently, future probes will be fabricated with internal grounding.

d. Neutron Imaging. The neutron radiographic facility at JUGGERNAUT reactor is now arranged to provide a neutron beam having a maximum intensity diameter of $6\frac{3}{8}$ in. Additional scatter problems produced by this larger area beam have made it necessary to employ additional shielding. This has been provided by the construction of a heavy-density concrete wall and roof. With this personnel shield in place, it is planned to determine the optimum graphite thickness in the beam path. Thermal neutron intensity, cadmium ratio, and radiographic resolution will be studied as a function of graphite thickness. Preliminary data gathered thus far indicate that the optimum thickness will be less than the 15 in. used in the initial beam configuration.

e. Application of Infrared Radiation. Investigation of the possible use of infrared radiation in nondestructive testing has continued. A Schmidt mirror optical system from an infrared snooperscope has been modified for use with an indium antimonide P.E.M. detector. The image focused on the detector is reduced by $\frac{1}{2}$ in. in size. The sensitive area of the detector is 2.4 x 1.35 mm; therefore the surface temperature of the object is averaged over an area of 4.8 x 2.7 mm on the object. The infrared radiation is chopped by a rotating disk with four holes spaced 90° apart, giving a chopping frequency of 240 cps. The signal from the detector preamplifier is filtered by a continuously variable electronic filter which is connected as a bandpass filter and adjusted for a bandpass of 240 ± 10 cps. An oscillator signal passed through the filter was attenuated by one-half at 170 cps and 330 cps. A tuned amplifier described in a G.E. report for use with a PbS infrared cell had a gain of 4×10^5 at 396 cps and a gain of 3×10^2 at 350 cps. A sharply tuned amplifier of this type would help to eliminate much of the noise in the signal. With the present system, temperature differences of approximately 3°C at 300°C can be detected.

4. Development of Extrusion Techniques

Three extrusions were made using the DPM (disposable particulate matter) extrusion technique (see Progress Report for November 1962, ANL-6658, p. 48). The clad and central core materials were Type 304 stainless steel with an Al_2O_3 powder annulus. In two billets, a thin wall sleeve of refractory metal (molybdenum in one billet, tantalum in the other) was located against the ID of the clad material. While the two billets extruded satisfactorily, a metallurgical bond was achieved only at localized areas, and the sleeve ID showed considerable raggedness because of imbedding of the powder from the annulus into the relatively soft sleeve. Further work will be done on extrusion of duplex tubing and other metals.

C. Chemical Separations

1. Chemical-Metallurgical Process Studies

a. Chemistry of Liquid Metals. Additional data for the yttrium-zinc system have been obtained by means of the recording effusion balance in experiments performed at 540°C. An effusion cell with extremely small orifices (0.004-in. diameter) was used in these runs in order to obtain greater accuracy in the location of the phases. In addition to the phases YZn_{12}, Y_2Zn_{17}, Y_2Zn_9, YZn_3, and YZn_2 previously indicated by effusion results obtained at 520°C (see Progress Report for December 1962, ANL-6672, p. 33), a phase having the composition YZn_5 was found to exist. Because of the extremely low evaporation rates beyond YZn_2, the effusion experiments were terminated before reaching the YZn phase, and consequently no direct observations of this phase were made.

The results obtained at Argonne are in general agreement with those of Chiotti,[7] who reported the existence of the following intermetallic compounds: YZn_{11}, Y_2Zn_{17}, YZn_5, YZn_4, YZn_3, YZn_2, and YZn. The ANL effusion data, which are supported by X-ray diffraction studies (see Progress Report for January 1963, ANL-6683, p. 39), suggest that the phases YZn_{11} and YZn_4 reported by Chiotti may correspond to the YZn_{12} and Y_2Zn_9 phases observed in the ANL study.

Studies of the technetium-zinc system were continued. A compact corresponding to a nominal technetium-to-zinc ratio of 20 was annealed for seven days at about 415°C. X-ray diffraction studies of the preparation showed that the technetium lattice parameters increased from a_0 = 2.735 Å and c_0 = 4.388 Å to a_0 = 2.799 Å and c_0 = 4.453 Å, thereby suggesting that a signficant solubility of zinc in solid technetium occurs.

b. Liquid Sodium Coolant Chemistry. The development of large fast-breeder power reactors is dependent on the use of liquid sodium for the transfer of heat from the reactor core to steam generators. As the trend toward increased power density of the reactor core and higher coolant temperature grows, the finding of materials of long-lasting integrity for the containment of liquid sodium will become more difficult.

The selection of suitable construction materials is made more difficult by the fact that the reactivity of liquid sodium is greatly enhanced by the presence of impurities, such as oxygen, in the sodium. Although considerable work has been done on the removal of oxide from liquid sodium by cold trapping and numerous material compatibility studies in liquid sodium have been made, the information available on the chemistry of liquid sodium under the conditions of its use as a coolant is incomplete.

---

[7] Chiotti, P., Mason, J. T., and Gill, K. J., Contribution No. 1218, Ames Laboratory, Ames, Iowa (1962).

The advancement of sodium-coolant technology depends largely upon the following: (1) the extent of knowledge of the chemical reactions between impurities in the sodium and materials of construction, (2) the ability to identify troublesome impurities and to establish their permissible levels, (3) availability of analytical methods for the measurement of the amounts of harmful impurities, and (4) availability of methods for the purification of sodium.

The reliability of analytical procedures will be the keystone in the solution of many of the chemical problems associated with the use of liquid sodium as a reactor coolant. Although a number of methods are available for the determination of oxygen with reasonable accuracy in concentrations above 100 ppm, none of the existing methods have high precision in the concentration range from 10 to 100 ppm, and none are of value below 10 ppm. One of the methods which is being explored for the analysis of oxygen is an activation method which involves the conversion of oxygen in the sodium to fluorine-18 by reaction of the oxygen with tritons. In this method, a small amount of lithium (about 0.1 percent) is alloyed with the sodium and the tritons are produced in situ by the $Li^6(n,T)He^4$ reaction. The utility of the method depends upon the production of a lithium-sodium alloy in which the lithium is uniformly dispersed throughout the alloy and in which the oxygen is not excessively segregated. Preliminary studies are under way to develop a method whereby lithium-sodium alloys possessing the requisite properties can be produced.

c. Reduction of Beryllium Fluoride. In two exploratory experiments, 52-g charges of beryllium fluoride in two different fluxes (equimolar calcium chloride-magnesium chloride and equimolar sodium chloride-potassium chloride) were reduced by zinc-magnesium alloy in air atmosphere at 750°C. Although the yields were low, it was shown that metallic beryllium can be produced by this technique. Studies of conditions and techniques to improve the yield are under way.

d. Reduction of Plutonium Dioxide. The reduction of plutonium dioxide (suspended in molten halide fluxes) by liquid magnesium-zinc alloys has been demonstrated in two series of runs performed on a 7-g plutonium oxide scale. In one series of runs, in which the flux composition was varied, the rate and extent of plutonium reduction did not seem to be highly sensitive to flux composition. This difference from thorium dioxide reduction behavior (see Progress Report for September 1962, ANL-6619, p. 25) and uranium oxide reduction behavior (see Progress Report for April 1961, ANL-6355, p. 30) may represent a method of separating plutonium from uranium and thorium, which may prove useful since uranium oxide-thorium oxide has been proposed as a reactor fuel.

In the second series of runs, the magnesium concentration in the magnesium-zinc alloy was varied. The distribution coefficients obtained in these runs (which utilized a 47.5 m/o calcium chloride-47.5 m/o magnesium chloride-5 m/o magnesium fluoride flux) were compared with distribution coefficients obtained using a pure magnesium chloride flux (Figure 7). The data suggest that the distribution coefficient is the factor which limits the extent of reduction and that the lower the magnesium chloride concentration in the flux, the less the plutonium loss in the flux. Work is progressing on retorting equipment to be used in recovering plutonium metal from the magnesium-zinc-plutonium ingots obtained in the reductions.

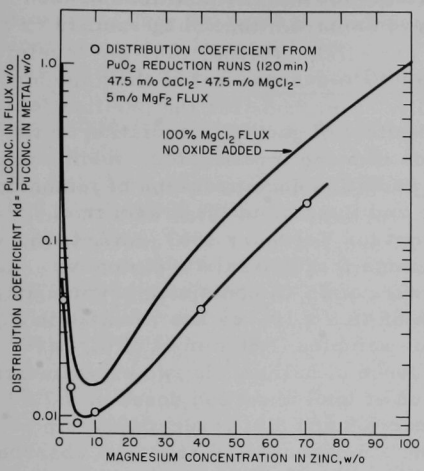

Figure 7. Distribution of Plutonium between Zinc-Magnesium Alloy and Fluxes Containing Magnesium Chloride

e. Molar Absorptivities of Uranyl(V) Chloride Spectra. Spectrophotometric studies were made of solutions in which uranyl(VI) chloride was thermally decomposed in molten chloride salt media at 650°C. The salt mixtures used were the eutectic lithium chloride-potassium chloride and the eutectic sodium chloride-potassium chloride-magnesium chloride. The spectrum obtained is attributed to the uranium(V) ion, UO_2^+. The pentavalent uranium species is believed to result from the reaction

$$UO_2Cl_2 \rightleftharpoons UO_2Cl + \frac{1}{2}\ Cl_2 \quad .$$

Molar absorptivities have been calculated for the uranium(V) species in both salt mixtures. Values for the major peaks are listed below:

$NaCl-KCl-MgCl_2$ Eutectic		LiCl-KCl Eutectic	
Wavelength ($m\mu$)	Molar Absorptivity (ϵ)	Wavelength ($m\mu$)	Molar Absorptivity (ϵ)
690	6.6	630	8.9
860	10.1	800	15.8
1520	16.7	1530	14.7
1610	6.2	1610	5.4

The main features of the spectra are the same in each of the solvents. The variations in relative intensities and the positions of the peaks result from the effects of the solvents on the absorbing species.

2. Fluidization and Volatility Separations Processes

a. Fluoride Separations. The effect of gamma irradiation on the decomposition of plutonium hexafluoride is being investigated. Additional data have been obtained on the gamma radiation decomposition of plutonium hexafluoride to plutonium tetrafluoride and fluorine in the presence of krypton and helium (see Progress Report for February 1963, ANL-6698, p. 47). An additional experiment on gamma irradiation of a plutonium hexafluoride sample (~80 mm Hg pressure at 25°C) containing krypton at 2 atm and a total absorbed energy dose of 48.8 x 10^{20} ev has resulted in a G value[8] of 1.3. Plutonium hexafluoride samples (~80 mm at 25°C) have also been gamma irradiated in the presence of helium. In two experiments made with helium at one atmosphere and at total absorbed doses of 9.7 x 10^{20} and 16.5 x 10^{20} ev, the G values were 6.8 and 8.0, respectively. In one experiment made with helium at one atmosphere and at a total absorbed energy dose of 44.4 x 10^{20} ev, the G value was 5.1. In two experiments made with helium at two atmospheres and a total absorbed energy dose of 11.4 x 10^{20} and 33.2 x 10^{20} ev, respectively, the G values were 7.5 and 5.7, respectively. The results of these experiments and of previously reported experiments (see ANL-6698, p. 47) have shown that, at low pressures of added inert gas or at low levels of absorbed energy, plutonium hexafluoride samples when irradiated in the presence of inert gases behave much like samples of plutonium hexafluoride when irradiated alone (a G value of 7.5). The gamma radiation decomposition of plutonium hexafluoride samples appears to be effectively quenched when irradiated to higher levels of total absorbed energy or in the presence of inert gases at high pressure. The data obtained in these and previous studies are summarized in Table XVI.

Table XVI. Decomposition of Plutonium Hexafluoride by Gamma Radiation in the Presence of Various Gases

Pressure of Plutonium Hexafluoride: ~80 mm at 25°C

Gas	Pressure (atm)	Total Absorbed Energy (ev x 10^{-20})	G Value[a]	Gas	Pressure (atm)	Total Absorbed Energy (ev x 10^{-20})	G Value[a]
Helium[b]	1	9.1	8.9	Krypton[b]	0.03	16	6.4
Helium	1	9.7	6.8	Krypton[b]	0.5	34	4.3
Helium	1	16.5	8.0	Krypton[b]	0.25	25	3.7
Helium[b]	1	40.0	3.4	Krypton[b]	1	80	1.4
Helium	1	44.4	5.1	Krypton[b]	1	106	1.0
Helium	2	11.4	7.5	Krypton	2	48.8	1.3
Helium	2	33.2	5.7				
Helium[b]	2	40	1.8				

[a]Molecules decomposed per 100 ev of radiation.

[b]Results of previous experiments (see Progress Report for February 1963, ANL-6698, p. 47).

[8]Molecules decomposed per 100 ev of radiation.

b. Decladding of Fuel Elements by Fluid-bed Oxidation. The development of a fluid-bed oxidation method for the separation of uranium dioxide pellets from stainless steel cladding in typical fuel elements is continuing (see Progress Report for February 1963, ANL-6698, p. 50). In this method, the uranium dioxide is oxidized with air to a higher oxide (U_3O_8). The uranium dioxide pellets break into fragments because of the large internal stresses produced by the difference in densities of the two oxides (UO_2 and U_3O_8). The U_3O_8 fines produced in the oxidation zone of the two-zone oxidation-fluorination reactor are elutriated to the fluid-bed fluorination zone.

An engineering-scale run has been made in which $1\frac{1}{4}$-in.-long simulated fuel elements (stainless steel-clad uranium dioxide pellets) were oxidized with air. The results of this run showed that only 85.5 percent of the uranium dioxide was removed from the pellets charged in 14.7 hr at 450°C with air at a superficial gas velocity of 0.75 ft/sec and gas pulsing (10 pulses/min at a pulse duration of 1 sec). The yield of 85.5 percent was lower than anticipated. Complete removal of uranium dioxide was expected on the basis of extrapolating the results of uranium dioxide removals from previously reported runs (see ANL-6698, p. 50). The reason for the low removal rate is being studied.

c. Chlorination and Fluorination Steps in the Separation of Uranium from Zirconium Alloy Fuels. The development of a chlorination-fluorination scheme for reprocessing highly enriched uranium-zirconium alloy fuels was continued. The work is being conducted in a $1\frac{1}{2}$-in.-diameter fluid-bed reactor with the alloy submerged in a fluid bed of inert material (Alundum). The first of the current series of runs used a miniature multiplate alloy fuel subassembly, instead of the uranium-zirconium chips ($\frac{1}{8}$ to $\frac{1}{4}$ in. in size) previously used, in order to simulate the actual process column-to-fuel size relationship (see Progress Report for January 1963, ANL-6683, p. 43). The fuel subassembly consisted of three 1 w/o normal uranium-zirconium alloy plate sections clad with zirconium ($\frac{5}{64}$ in. thick by 1 in. wide by 5 in. long) which were spaced $\frac{1}{8}$ in. apart. The subassembly weighed 160 g and contained 1.98 g of uranium. The chlorination-fluorination sequence consisted of hydrochlorination followed by reaction with fluorine. A 15.3-hr run was made with this sequence. This run included 7.3 hr of reaction with hydrogen chloride at 400°C fluid-bed temperature, 4 hr of no reaction at 250°C during which time nitrogen was flowing through the fluid bed, 2 hr of fluorination with fluorine (65 volume percent) at 250°C, followed by two fluorination periods of 1 hr each with fluorine (65 and 95 volume percent, respectively) at 500°C. During the hydrochlorination step, the downflow filter bed of Alundum was maintained at 400°C. Following the hydrochlorination step, the filter bed only was fluorinated with fluorine (50 volume percent) for 4 hr at 250°C. The filter bed was removed during the subsequent fluorination of the fluid bed.

Of the initial uranium charge (1.98 g), a residual uranium content of 0.01 w/o was retained by the Alundum (Type RR, -40 +60 mesh) in the fluid bed, and 0.007 w/o by the Alundum (Type 38, -14 +20 mesh) in the filter bed. These residual uranium values were significantly lower than those obtained previously[9] and may be due to the modified fluorination procedure used in this run. (Fluorinations in previous runs were carried out at 450°C with fluorine concentrations of 2 to 4 percent.) Other uranium losses included 2.2 w/o through the filter to the zirconium tetrachloride condenser during hydrochlorination and 4.5 w/o to the alumina fluorine disposal trap downstream of the uranium hexafluoride collection cold traps during fluorination. A material balance showed that the remaining uranium (95 w/o) was collected in the cold traps as hexafluoride. Of the initial uranium charged, the major portion (67.4 w/o) of the uranium hexafluoride was collected during the initial low-temperature (250°C) fluorination period and a much lower, but significant amount (6.6 w/o) during the subsequent higher-temperature (500°C) fluorination period. The remainder of the uranium (26 w/o) was distributed in the filter bed, the alumina trap, and the Alundum beds. The separate fluorinations of the fluid bed and the filter bed showed that, after the hydrochlorination reaction step, about 80 percent of the uranium was associated with the fluid bed and about 20 percent of the uranium was associated with the filter bed. Inspection of the subassembly after the initial hydrochlorination period (2.5 hr) showed that 44 percent of the subassembly had reacted with the hydrogen chloride. The remaining portion of the subassembly was reacted with hydrogen chloride during the subsequent hydrochlorination period (4.8 hr). These reaction time periods were not optimum because a planned shutdown for examination of the subassembly was carried out after the initial hydrochlorination period.

d. Fluid-bed Hydrolysis of Zirconium Tetrachloride. An investigation of the fluid-bed hydrolysis (by steam) of zirconium tetrachloride to zirconium dioxide in a series of engineering-scale runs in a 6-in.-diameter column was concluded. Two final runs were made to determine the cause for the excessive production of fines (-200 mesh) noted in previously reported work (see Progress Report for February 1963, ANL-6698, p. 51). However, the results were inconclusive because of plugging of the gas inlet section in the fluid-bed column by, as yet, unidentified, unsublimable solid residue present in the zirconium tetrachloride. It is possible that this unsublimable solid residue may be a source of the fines or a contributing factor to fines production. Further studies of the hydrolysis of zirconium tetrachloride will be made in the pilot plant which is now under construction. Engineering-scale work is underway on the fluid-bed hydrolysis of aluminum tetrachloride, which is a corresponding waste material from the processing of aluminum-based fuels.

---

[9]See Chemical Engineering Division Summary Report April, May, and June 1962, ANL-6569, pp. 113 ff.

e. Conversion of Uranium Hexafluoride to High-density Uranium Dioxide. A fluid-bed method for preparing high-density, spheroidal uranium dioxide particles directly from uranium hexafluoride involves the simultaneous reaction of the uranium hexafluoride with steam and hydrogen in the region from 650 to 700°C. Uranium dioxide with particle densities of up to 89 percent of theoretical density have been produced directly at 700°C; final particle densities of 96.5 percent of theoretical density were obtained by sintering in hydrogen at 1725°C.

Current work studied the course of the increase in density of a starting bed of relatively low-density uranium dioxide. The run was made without the addition of seed particles. The starting bed was low-density (6.7 g/cc) uranium dioxide particles (-20 +325 mesh). The run was carried out in three periods of operation at a reaction temperature of 650°C: pretreatment of the uranium dioxide starting bed with steam and hydrogen for 5 hr, followed by two uranium hexafluoride-feed periods of 3 and 5 hr each. The steam and hydrogen rate were about 1.3 and 15 times the stoichiometric requirement,[10] respectively. The uranium hexafluoride feed rate was 25 g/min (30 min/hr feed time). In the cleanup period (30 min/hr) to complete the conversion of uranium hexafluoride to uranium dioxide, only steam and hydrogen were fed at a combined superficial gas velocity of 1.0 ft/sec. The density of the starting bed increased from 6.7 to 6.9 g/cc during the pretreatment step with steam and hydrogen and increased further to a final density of 8.6 g/cc (in almost a straight-line fashion) during the two uranium hexafluoride feed periods. The high density (8.6 g/cc) and low rate of particle growth of the uranium dioxide particles indicated that a sintering mechanism between the starting-bed material and the deposited material could be responsible for the increase in density of the starting bed material.

3. Calorimetry

Calorimetric combustions of niobium in fluorine have been completed. Analytical work and auxiliary studies are in progress.

A technique has been developed for eliminating the oxide impurity from ZrF_2 and CdF_2, which are used as support discs for low-melting substances. The technique consists of treating the fluoride with liquid fluorine at 250°C and ~100 atm for 15 hr. Elimination of the oxide avoids an oxygen correction in calorimetric determinations.

Techniques for the combustion of uranium monosulfide in fluorine are being developed in preparation for the determination of the heat of formation of uranium monosulfide.

---

[10] Based on the reaction $UF_6 + 2H_2O + H_2 \rightarrow UO_2 + 6HF$.

IV. PLUTONIUM RECYCLE PROGRAM

A. Core Design

The irradiation of an experimental core in the EBWR is part of the program planned for the Plutonium Recycle study. A three-zone core is being designed and will consist of 36 plutonium fuel elements (fuel composition: 2.5% PuO_2-97.5% $U^{238}O_2$) in the central zone, which is surrounded by a single row of enriched uranium fuel elements to form the shim or driver zone, and a third zone of natural uranium fuel elements to form the blanket. The shim zone will be replaced periodically to provide the necessary reactivity for long (burnup) irradiations.

New multigroup cross sections have been derived for use with europium-samarium burnable poisons in the shim zone of the EBWR plutonium recycle core (see Progress Report for February 1963, ANL-6698, p. 53). The cross sections were obtained for the spectrum in the plutonium zone having a void fraction 0.3 and with the europium and samarium concentrations corresponding to about 12 and 20 gm per fuel element, respectively. Both seven- and four-group cross sections were obtained, including sets appropriate for use with the two-dimensional PDQ code.

Resonance parameters for Pu^{240} are being inserted into the GAM-I code. These parameters will permit direct calculation of resonance self-shielding and allow for spatial heterogeneity. Previously, the self-shielding values were obtained by solving the homogeneous MUFT-IV code, but comparison with experimental results have indicated that neglect of the spatial heterogeneity factor may lead to significant errors.

The DSN code is being used to determine the thermal disadvantage factors for the plutonium zone, shim zone, and the natural uranium zone. New average regional voids predicted from the recent hydrodynamic results with pure scattering in the reflector region suggested by Honeck[11] are being used in the calculations.

---

[11] H. C. Honeck, Some Methods for Improving the Cylindrical Reflecting Boundary Condition in Cell Calculations of the Thermal Neutron Flux, Trans. Amer. Nuclear Soc., 5, 350 (1962).

V. ADVANCED SYSTEMS RESEARCH AND DEVELOPMENT

A. Direct Conversion Studies

1. Direct Conversion by Thermionic Emission with a Cesium Cell

A new thermionic, electrically heated test cell was constructed to permit the emitter-collector distance to be varied over a distance of 13 mm. The collector is mounted on a bellow and is moved by an external micrometer head. The cell is equipped with a tantalum emitter and a molybdenum collector which is surrounded by a guard ring.

The cesium trap and the cell were placed inside of a thermostatically controlled oil bath. Its temperature varied from 30°C to 200°C and the cesium pressure from about 10^{-5} to 10^{-1} mm. The cell is now undergoing performance tests. The current-voltage characteristics were traced with an X-Y recorder.

The observed saturation currents of the tantalum emitter were compared with the theoretical values given in the literature, using the constants A and Φ from Richardson's equations, where

$$A = 37.2 \text{ amp/cm}^2 \quad ; \quad \Phi = 4.1 \text{ ev} \quad .$$

The black-body emitter temperature was observed inside a hole in the emitter through a sapphire window. It was found that the theoretical current values and the observed current values with zero voltage between collector and grounded emitter agreed quite well as long as the current remained essentially constant between -2 to +5 v at the collector. As soon as the values digressed, rf voltages were observed and the current fell far below the theoretical saturation values. The change determined the transition point between the ion-rich or neutral plasma condition to the electron-rich or space-charge-limited condition.

Following the procedure described in R.F. Oscillations and Power Output in Alkaline Thermionic Converters, by Hans K. Richards, Advanced Energy Conversion, Vol. 2 (1962), the cell characteristics were plotted with: rf voltages open, marked "O"; and rf voltages short circuited, marked "S." The rf output was separated from the dc component by inserting a 2-μF capacitance. An rf choke was included in the dc section to exclude the rf output. The dc characteristics depend very little on the open or the short-circuited rf when the rf voltage is low. As soon as the rf voltages increased, the dc characteristics varied considerably with rf, either at "O" or "S." In some cases, with rf "O," the curves showed considerably lower dc currents than rf "S." As observed previously, the rf usually decreases with decreasing voltage at the collector with the emitter

grounded. However, frequently the amplitudes of the harmonics increase with decreasing dc voltage and the original rf fundamental output disappears. This sometimes results in doubling the frequency.

The amplitude of the oscillations decrease rapidly with emitter collector distances of less than one millimeter. Additional experiments will be made in order to investigate this phenomenon further.

The rf power for a given spacing will first increase with increasing negative space charge and then reach a maximum ratio of rf/dc power before decreasing again. For 2-mm emitter-collector distance the rf/dc ratio reached 18%. At closer spacings, the rf power decreases rapidly.

2. Thermionic Energy-conversion Diode with a Film-boiling Liquid Metal

The previous design of the thermionic energy-conversion diode (see Progress Report for May 1962, ANL-6573, p. 46, Figure 4) with a liquid metal collector had been modified to eliminate leaks in the diaphragm. A disk of tantalum was welded to the top of the emitter to protect the center of the diaphragm from heating effects by the electron emitter. The change reduced the temperature of the diaphragm and, hence, the thermal stress. The change has increased the operating life of the diaphragm from about 8 hr to such a condition that operation for over 80 hr without failure has occurred.

Experiments were conducted to investigate the thermal conditions under which a stable film-boiling sheath is formed between the electron emitter and the liquid metal pool. Under these conditions the cell operates as a conversion diode. Data for potassium are shown in Figure 8. The emitter temperature is approximately 2035°K. The pool or electron collector temperature T_C is plotted as a function of the saturation temperature T_S which is fixed by the pressure of an argon blanket over the pool. On the diagonal line, the collector pool is at the boiling point. Starting at a point on the diagonal, if T_C is held constant and T_S is increased, the pool becomes subcooled. The numbers beside the data points give the maximum submersion of the emitter in the pool in centimeters which can be tolerated before a surface instability begins. The experimental conversion diode can operate for long periods of time to provide a steady dc output under the conditions indicated by any of the data points if the submersion is less than or equal to that shown.

When the maximum submersion is exceeded, three different types of limits are observed. In the region at the lower right, marked GS in Figure 8, the diode is intermittently shorted and unstable surface waves, i.e., of growing amplitude, are generated. In the central region SS, the diode is intermittently shorted and surface waves which are stable, i.e., not growing, are generated. In the region nearest saturation, GU, unstable

surface waves are generated which are large enough to modulate the electrical output characteristic, but do not short the diode. With still deeper submersion, shorting occurs. Data points which are on the boundary between two regions are indicated by diamonds. Places where the boundary is not well defined by the data are indicated by a dashed line. The highest temperature for the potassium pool in this apparatus is established by the excessively high decomposition rate of the silicone oil coolant at temperatures above 650°K.

The data indicate dc power is best generated with a liquid potassium diode when it operates in the SS region.

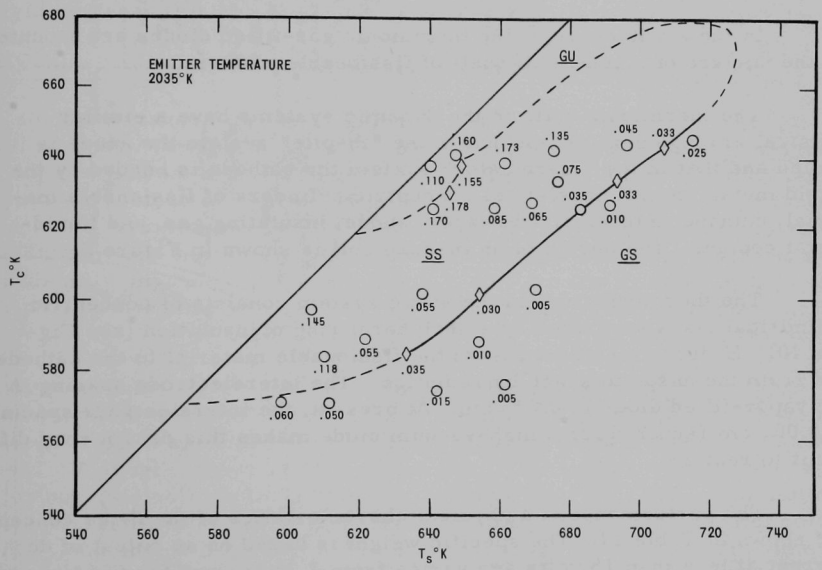

Figure 8. Collector Temperature (T_C) vs Potassium Saturation Temperature (T_S) for Maximum Emitter Submersion in Centimeters with Emitter Temperature about 2035°K

3. Nuclear Thermionic Power Systems

Three concepts of nuclear thermionic converters in the megawatt electrical range were investigated as possible sources of power for satellite stations and propulsion engines in electrically propelled rockets. Two concepts are designated as dynamic systems and one is designated as a static system. For these applications the specific weight, kg/kwe, is critical.

This study is based on improvements in technology which are anticipated to occur within the next decade. Basically, the study reflects the performance possible with collector temperatures of 1400-1600°K, which are higher than practical in current technology. In the two dynamic concepts, a liquid metal is used to transfer heat from the nuclear reactor to the radiator. In the "in-core" dynamic concept, the liquid metal is used to transfer the sink heat from the anode of a gas-filled diode located in the core to the radiator. In the "in-radiator" dynamic concept, the liquid metal is used to transfer the heat from the reactor to the cathode of a gas-filled diode located in the radiator, and the sink heat is radiated from the anode to space.

In the static concept, the thermionic gas-filled diodes are mounted on the surface of a spherical shell of fissionable material.

The thermionic cells in the dynamic systems have a similar physical arrangement except that in the "in-pile" system the anode is cooled and that in the "in-radiator" system the cathode is headed by the liquid metal. A cell consists of concentric cylinders of fissionable material, cathode, interelectrode vapor, anode, insulating gas, and liquid-metal coolant. The design of an in-core cell is shown in Figure 9.

The thermionic cell in the static system consists of concentric cylindrical discs separated by a peripheral ring of insulation (see Figure 10). Heat is transferred from the fissionable material to the cathode and from the anode to space by radiation. The interelectrode spacing in the vapor-filled diode is 0.025 cm. At present, the interelectrode spacing of 0.001 cm required for a high-vacuum diode makes this design very difficult to realize.

The performance and physical characteristics of the three concepts are shown in Table 17. The specific weight is based on an output of dc current at less than 15 volts and varies from 2.76 kg/kwe for the "in-core" dynamic concept to 5.14 kg/kwe for the static concept.

B. Rocket Fuel Test Reactor (RFTR)

As part of a study to develop nuclear propulsion systems for rockets, two methods for testing fuel elements under design conditions are being investigated. The incentives for utilizing such systems are to reduce testing time and to overcome the limitations of electrically heated test rigs without going to the expense of full-core experiments.

For the purpose of this study, the assumption is made that advanced rocket reactor cores may operate at power densities up to 10 Mw/liter and a reasonable test volume is taken to be 20 liters.

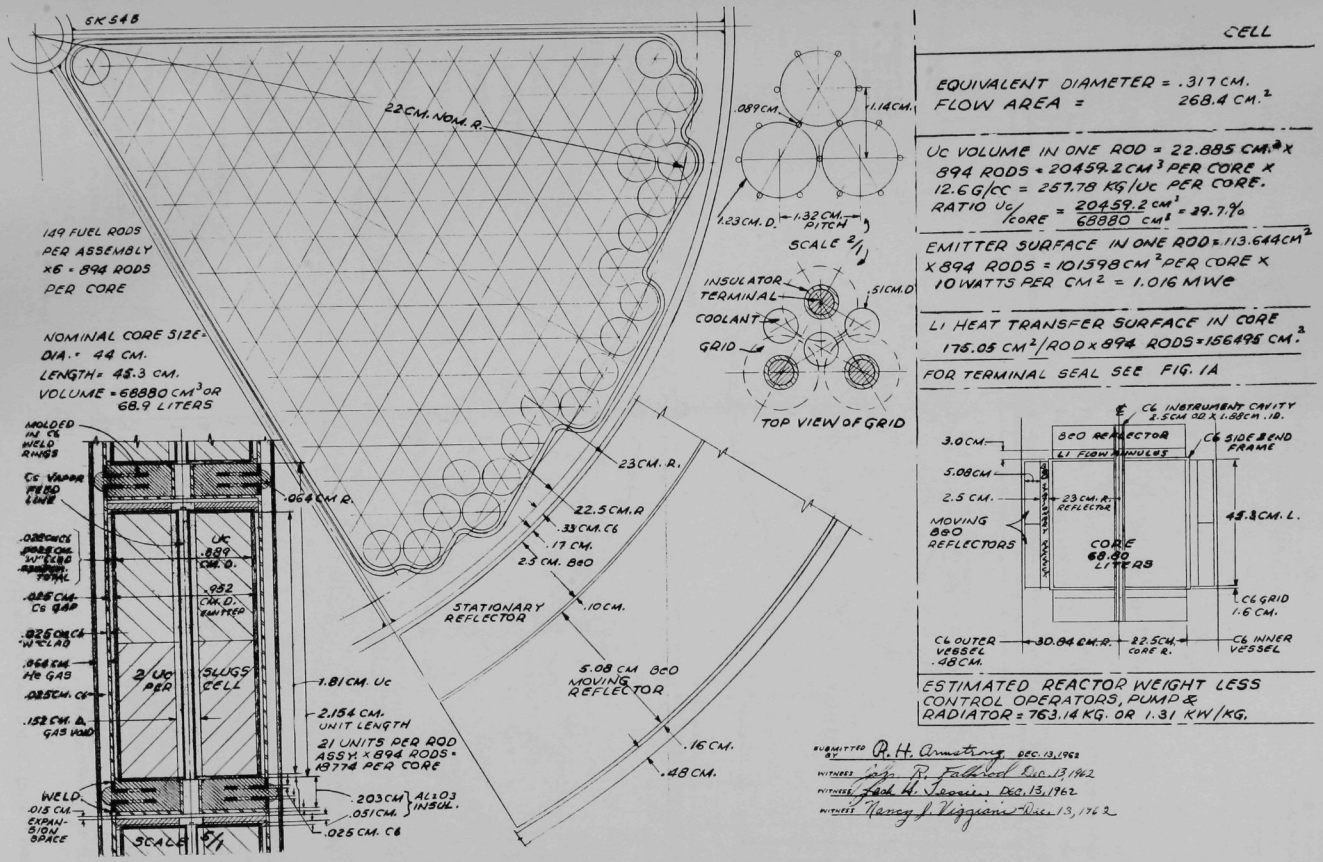

Figure 9. The Design of a Gas-filled Thermionic Cell Used In a Liquid Metal-cooled (dynamic) Reactor System

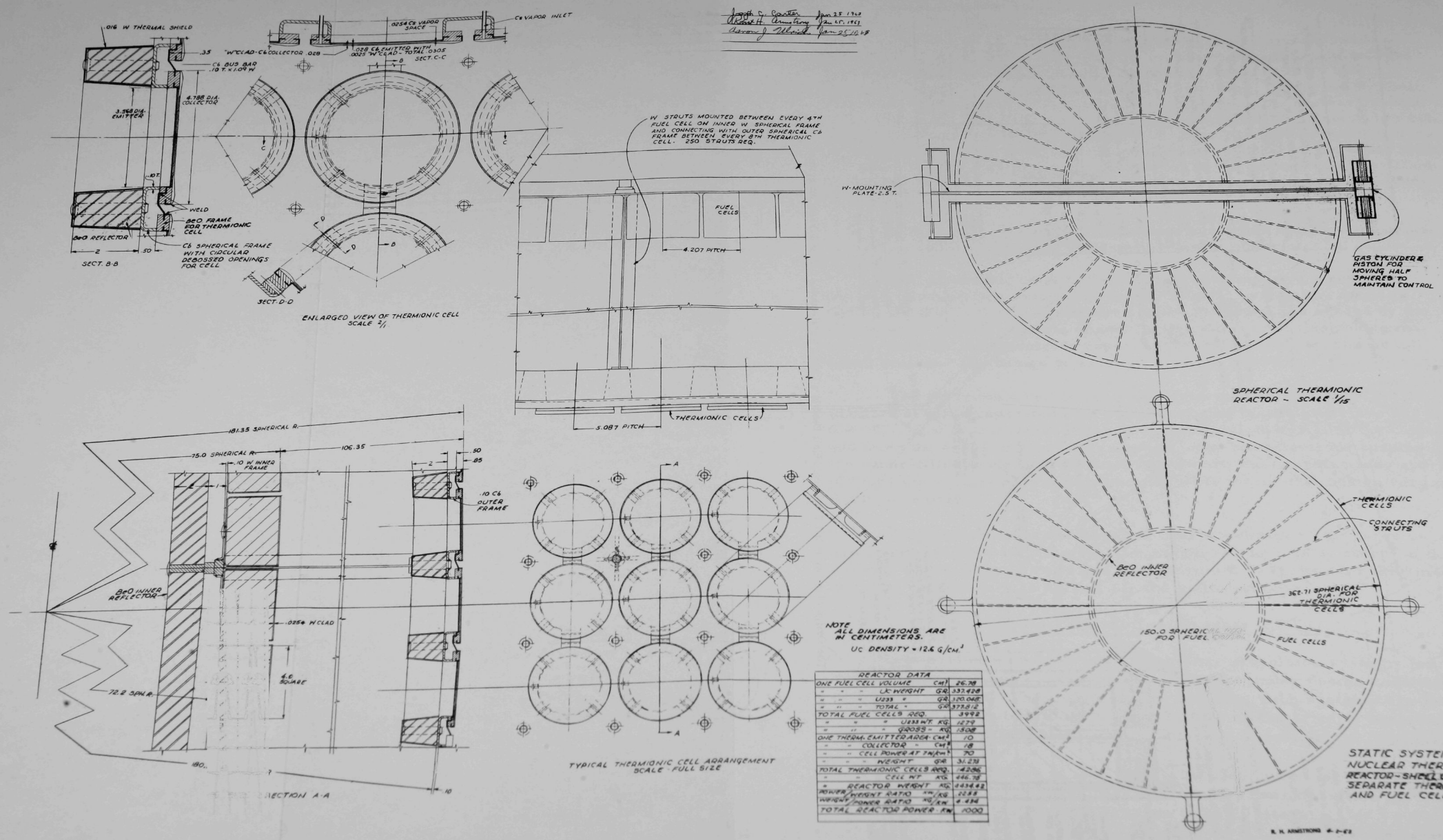

REACTOR DATA		
ONE FUEL CELL VOLUME	CM³	26.38
" " " UC WEIGHT	GR.	337.428
" " " U233 "	GR.	320.065
" " " TOTAL "	GR.	373.612
TOTAL FUEL CELLS REQ.		3992
" " " U233 WT.	KG.	1272
" " " GROSS "	KG.	1508
ONE THERM. EMITTER AREA	CM²	10
" " COLLECTOR "	CM²	18
" " CELL POWER AT 7W/cm²		70
" " " WEIGHT	GR.	31.231
TOTAL THERMIONIC CELLS REQ.		4296
" " CELL WT.	KG.	446.78
" REACTOR WEIGHT	KG.	1434.42
POWER/WEIGHT RATIO	KW/KG.	1.238
WEIGHT/POWER RATIO	KG/KW.	1.434
TOTAL REACTOR POWER	KW.	1000

Figure 10. The Design of a Gas-filled Thermionic Cell Used in a Convection (static) Cooled Reactor System

Table XVII. Performance Data

Concept Number	1	2	3
System			
Physical Arrangement	diodes in reactor core	diodes in radiator	diodes on spherical shell
Type of System	dynamic	dynamic	static
Electrical Rating, kw	1000	1000	1000
Efficiency, %	10	8	10
Voltage, v	14.7	14.7	14.7
Current, amp x 10^{-3}	69	69	69
Specific Weight, kg/kwe	2.76	2.93	5.14
Reactor			
Type	fast	fast	fast
Core Geometry	heterogeneous cylinder	heterogeneous cylinder	hollow sphere
Fissionable Material	U^{235}	U^{235}	U^{233}
Core Composition, %			
UC	32.08	51.67	85
Al_2O_3	19.07	-	-
Nb-1% Zr	25.26	20.36	-
Lithium	18.03	28.01	-
Tungsten	0.42	0	-
Voids and Cesium Vapor	5.14	0	-
BeO	-	-	12
Specific Weight, kg U/kwe	0.25	0.20	1.28
Cathode			
Fuel Temperature (max), °K	2600	2600	2600
Material	W on Cb-1% Zr	W on Cb-1% Zr	W on Cb-1% Zr
Temperature, °K	2100	1830	2100
Area, cm^2	5.4	16	10
Work Function, v	2.9	2.6	2.9
Interelectrode Gas			
Gas	Cs	Cs	Cs
Pressure, mm Hg	17	7	17
Electrode Spacing, cm	0.025	0.025	0.025
Anode			
Material	W on Cb-1% Zr	W on Ta	W on Cb-1% Zr
Temperature, °K	1600	1400	1600
Area, cm^2	5.7	16	18
Work Function, v	2.0	1.8	2.0
Cell Performance			
Voltage, v	0.7	0.6	0.7
Current, amp/cm^2	14.3	10	7.2
Power, w/cm^2	10	6	5

Various two-region systems, consisting of a uranium-fueled driver surrounding the test region, are being considered. In particular, the following combinations for the driver system appear interesting:

(1) sodium cooling and a lightly loaded uranium-zirconium matrix structure;

(2) sodium cooling with some beryllium moderator to yield an epithermal neutron spectrum;

(3) D_2O cooling and moderation with a fairly heavy uranium loading to yield a compact core and an epithermal spectrum.

These three systems have been studied in cylindrical geometry in some detail. Results obtained with the RE-122 code are being compared with results obtained from the DSN code to check the applicability of diffusion theory to these systems.

It is found that the neutron spectrum at the center of the test section (20-liter volume, 17-cm radius) is fairly independent of the driver composition. The spectrum at the outer edge, and hence the power peaking, however, is a strong function of the design of the driver region.

The second method being considered for testing fuel elements involves the use of a single-zone core similar to the desired rocket design having reduced critical-mass requirements. By altering the fuel concentration and composition, or by changing the reflector savings, it may be possible to "mock up" the design core with fewer fuel elements and thus reduce the fuel requirements. To explore reflector effects, some calculations in spherical geometry were made for an arbitrary test section having the following composition: 44% voids, 22% UO_2 (95% enriched), and 34% tungsten. The results are shown in Table XVIII.

Table XVIII. Results of RE-122 Calculations for Rocket Test Cores

Problem No.	Reflector Thickness (cm)	Reflector Composition	Critical Radius (cm)	Ratio of Power Densities Edge/Center	Total Core Volume (liters)
112	20	full-density Be	23	7.0	53
113	20	70% density Be	32	2.8	133
114	40	full-density Be	18	14.0	23
115	0	-	53	~cosine distribution	623

Problem 115 was recalculated to investigate the effect of hydrogen on criticality. The presence of gaseous hydrogen reduced the critical radius about 0.5 cm.

VI. NUCLEAR SAFETY

A. Thermal Reactor Safety Studies

1. Metal Oxidation and Ignition Studies

Studies were continued of the oxidation of uranium by air and of the role of nitrogen in the oxidation reactions. The experiments were carried out at temperatures of 600°C and above. The oxidation runs were made by passing air containing a small quantity (about 6 percent) of argon gas over one-cm cubes of uranium which were supported on thermocouples and heated to the desired temperature by an induction coil. After passage of the gas over the uranium, the gas was analyzed by a mass spectrometer for oxygen and nitrogen depletion at 5-min intervals. Initial oxidation rates were found to increase with temperature. It was found, however, that the protectiveness of the oxide film which was formed also increased with increasing temperatures, and that the rates of oxidation at 900 and 1000°C were less than those at 700 and 800°C after a period of time (about 15 min). Results indicated that nitrogen was not absorbed over the temperature range from 600 to 1000°C.

Since it was demonstrated that nitrogen was not absorbed during the reaction of uranium with air, a simpler and more rapid system of following the oxidation reaction could be devised. A natural-circulation loop has been constructed by means of which the reaction rate can be measured by observing the decrease in pressure in the system. The newly constructed apparatus is currently being used to study the initial stages of the oxidation reaction.

Further studies of the oxidation of plutonium by air have been carried out. Previously reported studies indicated a parabolic-linear rate up to 300°C, with activation energies of 32 kcal/mole for the parabolic portion of the rate curve and 16 kcal/mole for the linear portion of the curve. Above 300°C, a change in the kinetics of the reaction appears to take place, which results in the occurrence of a minimum in the rate at about 420°C. A series of oxidations of a cube of plutonium over the range from 340 to 480°C was performed with the use of a thermobalance. The results of the experiments clearly indicated a minimum at about 410°C. Runs made at 385°C and at 406°C yielded data that could be fitted equally well to a cubic or a parabolic rate law. The reason for this behavior is not yet clearly understood.

Preparations are being made to study the ignition behavior of plutonium and plutonium-alloy foils. The binary alloys of plutonium will contain the following alloying elements in concentrations of two atom percent: carbon, silicon, chromium, manganese, iron, cobalt, nickel, cerium, and uranium.

2. Metal-Water Studies

The apparatus for the isothermal study of the uranium-steam reaction by the volumetric method has been modified to allow studies of the reaction at higher temperatures. In the modified apparatus, a one-inch-diameter by $\frac{1}{4}$-in.-thick disk is supported on a flat quartz plate. Examination of the uranium disk after the run showed that the thickness of the oxide was the same on both of the flat surfaces of the disk, thereby implying that the quartz support did not interfere with the oxidation reaction.

Preparations are being made for the study of the reaction of small metal spheres (0.3 to 1.5 mm in diameter) with water while the spheres are submerged in water. The spheres will be heated by means of a light beam from a 30-joule laser. The extent of the metal-water reaction will be determined by measurements of the quantity of hydrogen produced and by metallographic studies of the oxide film thickness.

In-pile studies of metal-water reactions in TREAT were continued. Three experiments were performed with aluminum-uranium alloy plates. The three plates were subjected to reactor energies which were sufficiently high to result in peak temperatures above 1800°C. Under these conditions, it is expected that extensive metal-water reaction will occur. The results of these experiments will be reported upon completion of the analytical work.

B. Fast Reactor Safety Studies

1. Meltdown Experiments with Ceramic Fuel

Sintered ceramic fuel bodies characteristically have a high elastic modulus, a high thermal expansion, low strength, and low thermal conductivity. Various ceramic-fueled elements are being exposed in the TREAT reactor to study their behavior in transient tests. In particular, studies are being made of fuel movement prior to failure, during failure, as well as after failure, by reassembling or disassembling the fuel fragments.

Uranium sulfide ceramic is now being investigated. Five tantalum-clad uranium sulfide samples were exposed in transparent capsules in TREAT. Each element consisted of a half-length EBR-II Mark-I-size tantalum tube containing a stack of uranium sulfide pellets in argon gas pressurized to 1 atm. The irradiation conditions are given in Table XIX.

The samples are now being prepared for post-irradiation examination.

Table XIX. Irradiation History of Uranium Sulphide Fuel Pellets

Sample No.	Reactor Integrated Power (Mw-sec)	Maximum Recorded Cladding Temperature (°C)
1	43	1060
2	38	890
	60	1265
3	54	1200
	77	1720
4	95	2000
5	113	2390

2. In-pile Oxidation Studies

A study has been started to determine the particle-size distribution that occurs when reactor fuels are heated in flowing air in a reactor environment. The first sample for this study has been irradiated in TREAT. This sample was a 1.3145-g sample of a U-5% fissium pin, 20% enriched, suspended in a nickel screen basket in a BeO crucible. Air at 11 cfm, or a linear velocity of 8.5 ft/sec, and room temperature was passed over the pin during a 54-Mws transient. The capsule was equipped with 224-μ, 47-μ, 25-μ, 5-μ, and 1-μ filters. The exit gas stream was passed through a liquid nitrogen-cooled charcoal trap and then through an AEC-type absolute filter before exiting to the stack.

A thermocouple placed inside the nickel screen cage under the pin indicated a temperature of 1290°C before it failed, at which time approximately two-thirds of the total nuclear energy produced in the pin had been released. The nickel cage which was suspended inside the BeO crucible (2 in. in ID and 3 in. long) failed, and the pin dropped, hit the bottom of the crucible, and deformed extensively. Part of the residue appeared to be cylindrically shaped, indicating that the nickel cage probably was not completely destroyed. Preliminary analysis of the results are as follows:

On bottom of BeO Crucible	1.280 g
224-μ filter (Type 304 SS)	0.0222 g
74-μ filter (Ni)	0.0034 g
25-μ filter (Type 304 SS)	0.0069 g
5-μ filter (Type 304 SS)	$<$0.0010 g
	1.313 g

The amount of material present on the bottom of the crucible and on the screens was determined by colorimetric analysis. These values will be checked by gravimetric and radiochemical analysis.

VII. PUBLICATIONS

Papers

DETERMINATIONS OF THE TOTAL EMISSIVITY OF POLISHED AND OXIDIZED URANIUM SURFACES
Louis Baker, Jr., E. M. Mouradian, and J. D. Bingle
Nuclear Sci. and Eng. 15, 218-220 (February 1963). Letter.

INTERMEDIATE PHASES IN THE SYSTEMS La-Zn, Ce-Zn, Pr-Zn AND Nd-Zn
Ewald Veleckis, Irving Johnson and H. M. Feder
Abstracts of Papers Presented at Am. Chem. Soc. Meeting, Los Angeles, March 31-April 5, 1963. p. 15K.

THE ZINC-VANADIUM PHASE DIAGRAM
M. G. Chasanov, R. V. Schablaske, P. D. Hunt and B. S. Tani
Trans. Met. Soc. AIME 227, 485-488 (April 1963).

MORE ON FAST-CERAMIC-REACTOR SAFETY
C. E. Dickerman and David Okrent
Nuclear News 6, pp. 21-22 (March 1963). Letter.

ADDITIONAL HYDRODYNAMIC TEST DATA FROM EBWR AT POWERS TO 60 Mw
M. Petrick
Proc. Nuclear Superheat Meeting No. 7, Sioux Falls, South Dakota, September 12-14, 1962, COO-266 (also TID-7658, October 30, 1962, pp. 75-77).

AN ANALOG SIMULATION OF THE TRANSIENT BEHAVIOR OF TWO-PHASE NATURAL CIRCULATION SYSTEMS
R. P. Anderson, L. T. Bryant, J. C. Carter, and J. F. Marchaterre
Heat Transfer - Houston, Ed. L. Bernath
Chemical Engineering Progress Symposium, Ser. No. 41, Vol. 59, 1963, pp. 96-103.

TRANSFER FUNCTION SYNTHESIS AS A RATIO OF TWO COMPLEX POLYNOMIALS
C. K. Sanathanan and Judith Koerner
IEEE Trans. AC-8(1), 56-58 (January, 1963).

PLUTONIUM AS A FUEL FOR THE EXPERIMENTAL BREEDER REACTOR-II (EBR-II).
L. J. Koch
Proc. Conf. on Plutonium as a Power Reactor Fuel, Richland, Washington, September 13-14, 1962. HW-75007 (December 1962). pp. 16.1-16.23.

A GENERALIZED TREATMENT OF THE ECONOMICS OF PLUTONIUM AS A FUEL IN FAST REACTORS
L. E. Link
Proc. Conf. on Plutonium as a Power Reactor Fuel, Richland, Washington, September 13-14, 1962. HW-75007 (December 1962). pp. 20.1-20.16.

THE PHYSICS OF PLUTONIUM IN FAST REACTORS
David Okrent and F. W. Thalgott
Proc. Conf. on Plutonium as a Power Reactor Fuel, Richland, Washington, September 13-14, 1962. HW-75007 (December 1962). pp. 14.1-14.33.

CERTIFICATION OF ALGORITHM 96 - ANCESTER [Robert W. Floyd., Comm. ACM, June, 1962]
Henry C. Thacher, Jr.
COMM. ACM, Vol. 6, No. 3, pp. 104-105 (March, 1963).

TRENDS IN HOT CELL DESIGN (PANEL DISCUSSION)
M. J. Feldman, J. R. Lilienthal, A. R. Olsen, J. E. Dummer, R. C. Goertz, R. V. Steel and H. C. Duggan
Nucleonics 21 (3), 66-71 (March 1963).

IN-CORE INSTRUMENTATION DEVELOPMENT, BORAX-V
E. J. Brooks
Proceedings of the Nuclear Superheat Meeting No. 7, Sioux Falls, South Dakota, September 12-14, 1962. COO-266 (also TID-7658) (October 30, 1962). pp. 62-63.

BORAX-V OPERATING EXPERIENCE
J. D. Cerchione
Proceedings of the Nuclear Superheat Meeting No. 7, Sioux Falls, South Dakota, September 12-14, 1962. COO-266 (also TID-7658) (October 30, 1962). pp. 48-50.

BORAX-V COLD CRITICAL EXPERIMENTS
J. I. Hagen
Proceedings of the Nuclear Superheat Meeting No. 7, Sioux Falls, South Dakota, September 12-14, 1962. COO-266 (also TID-7658) (October 30, 1962). pp. 51-53.

STATUS OF BORAX-V OPERATION
R. E. Rice
Proceedings of the Nuclear Superheat Meeting No. 7, Sioux Falls, South Dakota, September 12-14, 1962. COO-266 (also TID-7658) (October 30, 1962). pp. 46-47.

PREPARATION AND SOME PROPERTIES OF ARC-CAST PLUTONIUM MONOCARBIDE
O. L. Kruger
J. Nuc. Matls. 7 (2) 142-150 (November 1962).

PHASE STUDIES ON ARC-MELTED PLUTONIUM-CARBON ALLOYS NEAR THE MONOCARBIDE COMPOSITION
O. L. Kruger
J. Am. Cer. Soc. 46 (2) 80-85 (February 1963).

STATUS OF BORAX-V SUPERHEAT FUEL FABRICATION, INSPECTION AND ASSEMBLY
W. C. Kramer
Proceedings of the Nuclear Superheat Meeting No. 7, Sioux Falls, South Dakota, September 12-14, 1962. COO-266 (also TID-7658) (October 30, 1962). pp. 18-22.

EFFECTS OF OXYGEN AND SURFACE TREATMENT ON THE CORROSION OF STAINLESS STEEL IN SUPERHEATED STEAM
W. E. Ruther and Sherman Greenberg
Proceedings of the Nuclear Superheat Meeting No. 7, Sioux Falls, South Dakota, September 12-14, 1962. COO-266 (also TID-7658) (October 30, 1962). pp. 6-8.

PLUTONIUM FUEL PROGRAMS AT ARGONNE NATIONAL LABORATORY
F. G. Foote
Proc. Conf. on Plutonium as a Power Reactor Fuel, Richland, Washington, September 13-14, 1962. HW-75007 (December 1962). pp. 7.1-7.21.

ANL Reports

ANL-6107 FABRICATION OF THE FUEL AND BLANKET FOR THE FAST SOURCE REACTOR (AFSR)
W. R. Burt, Jr.

ANL-6276 FABRICATION OF EBR-II, CORE I FUEL ELEMENTS
N. J. Carson, N. R. Grant, N. F. Hessler, H. F. Jelinek, R. H. Olp, and A. B. Shuck

ANL-6489 THE FACILITY 350 HELIUM-ATMOSPHERE SYSTEM
R. M. Mayfield, W. G. Tope, and A. B. Shuck

ANL-6606 A FLUID-BED PROCESS FOR THE DIRECT CONVERSION OF URANIUM HEXAFLUORIDE TO URANIUM DIOXIDE
I. E. Knudsen, H. E. Hootman, and N. M. Levitz

ANL-6640 PROCEEDINGS OF THE AMU-ANL SUMMER STUDY PROGRAM, June 19-July 14, 1961
Amended Notes Edited by C. V. Pearson from Original Notes
Compiled by G. E. Schweitzer

ANL-6660 THE AXISYMMETRIC FREE-CONVECTION HEAT TRANSFER ALONG A VERTICAL THIN CYLINDER WITH CONSTANT SURFACE TEMPERATURE
R. Viskanta

ANL-6661 CALCULATIONS FOR ZPR-VII UNIFORM LATTICE CRITICAL EXPERIMENTS WITH THORIA-URANIA FUEL IN HEAVY WATER
E. M. Pennington

ANL-6674 REDUCTION OF VAPOR CARRYUNDER IN SIMULATED BOILING
P. L. Miller and C. P. Armstrong

ANL-6692 A RETROSPECTIVE ANALYSIS OF ASPECTS OF THE ALPR (SL-1) DESIGN
W. J. Kann and D. H. Shaftman

ARGONNE NATIONAL LAB WEST
3 4444 00008894 8